TECHNICAL PAPER

Study on delamination factor and surface roughness in abrasive water jet drilling of carbon fiber-reinforced polymer composites with different fiber orientation angles

Meltem Altin Karataş[1] · Ali Riza Motorcu[2] · Hasan Gökkaya[3]

Abstract

Carbon fiber-reinforced polymer (CFRP) composites are used in aerospace applications because of their superior mechanical properties and light weight. Avoiding damage in the machining of CFRP composites is difficult using traditional methods. Abrasive water jet (AWJ) has recently become one of the preferred machining methods for CFRP composites. This study evaluated the AWJ machinability of CFRP composites having three different fiber orientation angles (M1: [0°/90°]s, M2: [+45°/−45°]s, and M3: [0°/45°/90°/−45°]s) according to the delamination factor (D_f), and the average surface roughness (R_a) as quality characteristics of the drilled holes. The aim of the study was to investigate the effects of different levels of AWJ drilling parameters on the delamination factor and surface roughness and to determine the optimum drilling parameter levels that provide minimum delamination formation and surface roughness values. For this purpose, AWJ drilling experiments were carried out using the Taguchi L16 (4^4) orthogonal array. Water pressure (WP), stand-off distance (L), traverse feed rate (F), and hole diameter (D) were chosen as process parameters. Analysis of variance was used to determine the percentage effects of the AWJ drilling process parameters. The microscopic surface roughness and delamination formation properties of the machined surfaces were revealed using a scanning electron microscope and an optical microscope, respectively. The most effective parameters on D_f and R_a in the AWJ drilling of M1, M2 and M3 CFRP materials were determined to be water pressure, and stand-off distance. Minimum D_f and R_a values were obtained when AWJ drilling the M3 CFRP composite with a fiber orientation angle of [0°/45°/90°/−45°]s. Minimum delamination formation and very good surface quality can be obtained when the optimum process parameters determined in this study are used in the planning process for the AWJ drilling of CFRP composites having different fiber orientation angles.

Keywords Carbon fiber-reinforced polymer (CFRP) composite · Abrasive water jet (AWJ) · Drilling · Delamination factor · Surface roughness · Process parameters · Taguchi method

Technical Editor: Lincoln Cardoso Brandao.

✉ Meltem Altin Karataş
   meltemaltin@ibu.edu.tr

1   Machinery and Metal Technology Department, Gerede Vocational School, Bolu Abant Izzet Baysal University, 14900 Bolu, Turkey

2   Industrial Engineering Department, Engineering Faculty, Canakkale Onsekiz Mart University, 17100 Canakkale, Turkey

3   Mechanical Engineering Department, Engineering Faculty, Karabük University, 78050 Karabük, Turkey

1 Introduction

Although carbon fiber-reinforced polymer (CFRP) composite materials have low density, they are harder than titanium. If proper fiber orientation angles (FOAs) are used, these composites have good fatigue strength, good creep and abrasion resistance, a low friction coefficient, high toughness values and low damage tolerance, chemical and dimensional stability, corrosion resistance, low electrical resistance, and vibration damping capabilities. All these excellent properties make this an attractive material [1, 2]. These CFRP composites find wide application in the aerospace, defense, shipbuilding, automobile, machine tool, sports equipment, power generation, and oil and gas industries, as they have high strength, high specific hardness, and low thermal expansion,

and because they provide high suspension [3–5]. In recent years, these composites have been used more widely in aircraft materials and for industrial purposes such as medical equipment [6].

The CFRP composite materials consist of different layers, and these layers can be of different materials or of the same material in different orientations [7]. The strength and hardness of such materials depend on how the FOA is arranged. Changes in the FOA lead to changes in the behavior and strength of the material at different angles [8]. The fibers in a unidirectional material extend in one direction and the strength and stiffness are only in the direction of the fiber. The fibers in a bidirectional (i.e., at 90° angles) material extend in two directions. The orientation of these layers has power in both directions; however, the force is not always the same [8]. They exhibit the properties of an isotropic material in the quasi-isotropic direction (at 0°, −45°, 45°, and 90° or at 0°, −60°, and 60° angles). Many composites used in the aerospace sector are produced from materials with quasi-isotropic structures [8].

Composite materials are among the types of materials that are difficult to process due to their inhomogeneous structure. Regardless of whether manufacturing is carried out with traditional or modern production methods, all layered composites undergo some damage including matrix errors (gaps, porosity), fiber cracks, interface cracks, fiber shrinkage/contraction, and delamination (hole surface damage). Generally, modern manufacturing methods are characterized by high specific energy and low metal removal rate compared to traditional manufacturing methods. Issues such as higher-dimensional accuracy, good surface finish in complex geometries, lack of the need for cutting tools, and absence of burrs in the finished workpiece are seen as the advantages of modern manufacturing methods over traditional methods [7]. However, delamination has been reported as the most serious damage caused during the machining of composite materials by both conventional and modern manufacturing methods [9].

Drilling is one of the most commonly used machining methods for the assembly of parts in the aerospace industry and has been reported to account for 40% of all machining operations [10]. However, because of the presence of two or more phases, the machining process for CFRP composite material is considered to be different from that of homogeneous chip removal for conventional materials [4, 11]. Any surface damage on the composites has a significant effect on product quality, and thus on-going studies are being carried out to prevent or reduce surface damage [12]. It has been stated in these studies that hole surface quality (surface roughness and dimensional accuracy) is affected by the cutting parameters, tool geometry, and cutting forces [8, 13]. Therefore, the correct selection of cutting parameters is of great importance in the machining of CFRP composites. Typical problems associated with surface integrity are encountered when machining CFRP composites with conventional cutting tools [14]. Many manufactured parts are rejected because of various types of damage such as fiber withdrawal, fiber breakage, matrix plastering, and delamination [15]. In the aircraft industry, it has been reported that 60% of parts are rejected during final assembly due to delamination damage [16]. In addition, the size of the spindles of the monolithic tools makes it impossible to reach narrow spaces as required; however, cutting tool wear also causes disruption of the work [14].

Abrasive water jet (AWJ) is one of the unconventional advanced hybrid manufacturing processes and has the potential for machining a wide range of materials, regardless of the type, compared to traditional manufacturing processes. Using different material and abrasive combinations, AWJ machining provides a variety of unique cutting features [17]. Abrasive water jet machining is a manufacturing process in which material is removed through wear [18]. The AWJ machining process is a combination of the machining principles of a water jet (WJ) and an abrasive jet (AJ) [17, 19]. This machining method is defined as a "cold" machining method which is unaffected by heat and demonstrates high flexibility, high machining variety, low machining forces, and lack of thermal degradation. It is known to have many advantages, especially in the machining of non-conductive, difficult-to-cut materials compared to cutting, turning, drilling, and milling [17]. The AWJ is a single-point tool that can be moved in any direction and is capable of cutting almost any material, with very little damage to the workpiece [20]. Compared to traditional machining processes such as two- and three-dimensional cutting, milling, turning, and drilling applications, AWJ can be used for a variety of machining procedures [7, 21]. With the use of the computer-aided design/computer-aided manufacturing (CAD/CAM) system, AWJ also has the capacity to shape complex three-dimensional parts [20].

Nowadays, research on the AWJ machining of different materials continues and successful results are being obtained [21]. Hashish emphasized that the use of CFRP composites is constantly increasing, and that AWJ is an ideal method for cutting this material. He stated that when cutting CFRP composite materials of five different thicknesses on the AWJ machine, the average surface roughness did not exceed 10 μm without delamination on the surface and that a maximum dimensional error of 0.25 mm was achieved [14, 22]. Shanmugam et al. [23] found that delamination did not occur on CFRP samples under the conditions of 345 MPa pressure, 0.5 mm/s traverse feed rate, and 6 g/s abrasive flow rate in the machining of CFRP composites using WJ alone and AWJ under different process parameters.

Phapale et al. investigated the effects of machining parameters on delamination formation in the AWJ drilling

of CFRP composite materials and the effects of different methods such as backing plate, pilot hole, and water immersion (under-water) drilling to control the delamination. The researchers found that delamination formation was prevented by using low water pressure and low abrasive flow rates and stand-off distance, in contrast to the high occurrence of delamination when using high water pressure and high abrasive flow rates and stand-off distance. In addition, the effect of the abrasive flow rate on the formation of delamination was reported. It was stated that the extent of the delamination was significantly reduced and the geometric accuracy of the holes was better when using delamination control techniques. They concluded that the surface quality of the holes drilled with AWJ improved when using low water pressure, stand-off distance and abrasive flow rates, and that the lowest roughness values were reached when drilling with a backing plate [24].

Miron et al. [25] obtained a high-dimensional accuracy of ± 0.05 mm and an average surface roughness of 7.243 μm in the AWJ cutting of CFRP composite material, and no delamination or abrasive residues were observed in the material. Wang and Guo [26] reported that delamination also occurred due to insufficient jet entry into the composite at low water jet pressure. Mayuet et al. [27] found that the most effective parameter in the formation of delamination was the abrasive grain. On the other hand, Miller et al. determined that a relatively irregular surface was formed when using a 720 mm/min traverse feed rate and 3.53 g/s abrasive flow rate, and that the best average roughness value was reached by using a 60 mm/min traverse feed rate and 9.78 g/s abrasive flow rate. They also found that delamination increased with increasing traverse feed rate [28]. Unde et al. cut CFRP composite with different fiber orientations using AWJ with different processing parameters and investigated the effects of the process parameters on the material removal rate (MRR), delamination factor, kerf width, and average surface roughness. They concluded that the stand-off distance and traverse feed rate affected the MRR, kerf width, delamination factor, and fiber orientation, and that the water pressure affected the average surface roughness. They stated that the CFRP composite material with 45° fiber orientation gave superior results compared to those with 60° and 90° orientations. They obtained an average surface roughness value of 4.911 μm in material with a fiber orientation angle of 45°, 4.927 μm with 60°, and 4.974 μm with 90° [18].

Jagadeesh et al. determined that the most dominant factors in minimizing surface roughness were the stand-off distance and traverse feed rate, based on their experimental study and statistical analysis of CFRP laminates to improve cut quality in AWJ machining. They stated that when increasing the traverse feed rate, the surface roughness also increased, and therefore, a lower traverse feed rate should be selected when surface quality is of great importance

[29]. Abidi et al. applied the AWJ drilling process to CFRP composite material under different process parameters and stated that the stand-off distance and abrasive flow rate were the main parameters affecting surface roughness. They concluded that using high and low traverse feed and abrasive flow rates would result in high surface roughness, and that minimal surface roughness would be achieved by using a low level stand-off distance along with medium traverse feed and abrasive flow rates [30]. Dhanawade and Kumar determined that the most important parameters for the control of surface roughness in the AWJ machining of CFRP composites were traverse feed rate and water pressure. The researchers stated that the surface roughness decreased with increasing water pressure and increased with increasing traverse feed rate. They also determined the minimum surface roughness value to be 2.742 mm. In addition, they also found that the surface roughness of the machined samples was improved by 10.75% using optimum process parameters levels, and that delamination and fiber retraction were prominent in the samples machined at low water pressure and high traverse feed rate [31].

In another study, Dhanawade and Kumar cut CFRP composites using AWJ and found that delamination decreased with increasing water pressure and abrasive flow rate and decreasing stand-off distance and traverse feed rate [32]. Dhanawade et al. observed delamination, embedded abrasive particles, and fiber withdrawal in the carbon epoxy composite samples machined via the AWJ process. They reported that surface roughness decreased with increasing water pressure and abrasive flow rate and decreasing stand-off distance and traverse feed rate [33]. Thongkaew et al. stated that the drilling of woven CFRP composite materials using AWJ caused more serious damage than the cutting process due to the jet's first contact with the material. It was determined that the water pressure was the main parameter affecting hole damage, and that the hole diameter would increase with the increase in water pressure, traverse feed rate, and stand-off distance. They concluded that CFRP composite material can be drilled without hole damage when machined using 110 MPa water pressure, 3.8 g/s abrasive flow rate, 1–2 mm stand-off distance, and 2 s drilling time. Similarly, they recommended using 200 MPa water pressure, 4 mm/s traverse feed rate, 7.0 g/s abrasive flow rate, and 2 mm stand-off distance for undamaged drilling with AWJ [34].

Kumar and Gururaja found that the average surface roughness increased with increasing traverse feed rate and decreased with increasing water pressure in the AWJ machining of titanium-carbon (Ti/CFRP/Ti) fiber-reinforced polymer hybrid composite material using different process parameters. They stated that better surface quality (3.827 μm) was achieved with 200 MPa water pressure, 237.693 mm/min traverse feed rate, and 1 mm stand-off distance [35]. Vigneshwaran et al., in their study on the

AWJ machining of fiber-reinforced composites, stated that AWJ parameters such as water pressure and abrasive flow rate are of great importance for delamination. They added that, although delamination could not be prevented, it could be significantly reduced under optimized or controlled operating conditions. They determined that the surface quality of the machined composites depended on various parameters, and that the surface roughness could be reduced by decreasing the stand-off distance and increasing the abrasive mass flow rate with the water pressure. They stated that the increase in stand-off distance and traverse feed rate would increase the surface roughness, but the striation on the cut surface could be reduced by using larger abrasive particles at an average traverse feed rate, high water pressure and a high flow rate [36]. Kale machined fiber-reinforced composite materials using AWJ and reported that the abrasive was the most important parameter in delamination formation, and that delamination could be eliminated by using optimized process parameters. He stated that delamination decreased with increasing water pressure, and increased with increasing traverse feed rate, stand-off distance, abrasive size, cutting depth, and abrasive flow rate. He found that the machined surface quality reduced with increased cutting speed, traverse feed rate, stand-off distance, abrasive size, depth of cut, abrasive flow rate, and water pressure [37].

Kim et al. investigated the effect of drilling parameters on delamination using eight different drilling methods in the AWJ machining of woven prepreg composite laminates under different process parameters. As a result of their experiment, they stated that delamination can be avoided by ensuring proper mixing of water and abrasive before reaching high water pressure. They proposed drilling the laminate composite with low water pressure and switching to high pressure for the rest of the cutting process [38]. Ramesha et al. stated that the traverse feed rate is the most important factor for surface roughness when machining GFRP composites with AWJ under different process parameters, and that the abrasive size, abrasive concentration and stand-off distance are not important for controlling the surface roughness [39]. The experimental study results of Prasad and Chaitanya regarding the machining of GFRP composites with AWJ revealed that the stand-off distance and fiber orientation were the main factors affecting the surface roughness. They determined that the surface roughness would increase with increasing water pressure. They stated that the abrasive flow rate would also reduce the surface roughness until it reached a certain limit. This was attributed to its ability to cut the material properly due to the high kinetic energy of more abrasive particles. They found that a better surface quality could be achieved with high water pressure, a high abrasive flow rate, a low stand-off distance, and a low fiber orientation angle [40].

Deepak and Davim stated that minimum surface roughness was achieved by using 150 MPa water pressure, 75 mm/min traverse feed rate, 14% abrasive concentration, and 3 mm nozzle stand-off distance when machining graphite-filled GFRP composites with AWJ. Furthermore, no delamination was observed when using optimal process parameters [41]. Deepak and Pai determined water pressure to be the most effective parameter on the hole diameter of graphite-filled glass epoxy laminates machined with AWJ using the optimum process parameters of 100 MPa water pressure, 1 mm stand-off distance, and 225 mm/min traverse feed rate. There was no delamination on the drilled hole surface; however, they reported that the impact of the jet caused damage to the hole edges [42]. Li et al. [43] observed fractured fibers and small gaps on the hole surface resulting from fiber retraction when drilling Ti6Al4V/CFRP hybrid stacks with AWJ. Kumar and Kant found that water pressure and traverse feed rate were the most important parameters, followed by stand-off distance and abrasive flow rate, affecting the surface roughness in the machining of Kevlar epoxy composite material with AWJ. They observed that surface roughness decreased with increasing water pressure and decreasing traverse feed rate [44]. Gupta achieved the minimum surface roughness value of 0.194 μm using the optimum machining parameters of 1.5 mm nozzle approach distance, 150 MPa water pressure, and 225 mm/min feed rate when machining zirconia (ZrO_2) ceramic composites with AWJ under different processing parameters [45]. Mohanraj et al. concluded that water pressure had a more significant effect on surface roughness than the abrasive flow rate and the stand-off distance in the machining of Aluminum 6061 material using AWJ. They found that the optimum machining parameter values for minimum surface roughness (0.41 μm) were 9 g/s abrasive flow rate, 40 MPa water pressure, and 3 mm stand-off distance [46]. Sankar et al. [47] reported the minimum surface roughness value to be 2.54 μm using the optimum process parameters of 200 MPa water pressure, 120 mm/min traverse feed rate, and 0.24 kg/min abrasive flow rate in the AWJ machining of Al6082 alloy.

In this study, the AWJ machinability properties of CFRP composites with three different fiber orientation angles (M1: $[0°/90°]_s$, M2: $[+45°/-45°]_s$, and M3: $[0°/45°/90°/-45°]_s$) were evaluated by investigating the delamination factor (D_f) and the average surface roughness (R_a) of the drilled holes. The aim of this study was to investigate the effects of process parameters on the delamination factor and average surface roughness of these three CFRP composites, and to determine the optimum process parameter values for the minimum delamination factor and average surface roughness. To achieve these goals, all steps of the Taguchi method were carried out [48–50]. Analysis of variance (ANOVA) was used to determine the percentage of the effects of the drilling parameters [50]. The delamination

formations and surface roughness of the holes were investigated using a scanning electron microscope (SEM) and an optical microscope to determine the microscopic properties. It is thought that the findings of this study and especially the determined optimum process parameter levels will contribute to the production of higher quality parts manufactured via AWJ machining of CFRP composites with different fiber orientation angles.

2 Materials and methods

This study investigated the AWJ drillability of CFRP composite materials having [0°/90°]s, [+45°/−45°]s, and [0°/45°/90°/−45°]s fiber orientation angles. The optimum levels of control factors providing a minimum delamination factor (D_f) and minimum average surface roughness

(R_a) values were determined by following the experimental and statistical procedures given in Fig. 1 step-by-step in the AWJ drilling of these three CFRP composites.
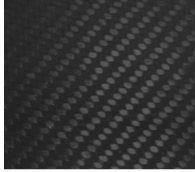
2.1 Workpiece

In this study, CFRP composites having three different fiber orientation angles (FOAs) that are widely used in the aerospace industry were used as experimental workpieces. The codes for the CFRP composite materials used in the AWJ drilling tests were M1 ([0°/90°]s), M2 ([+45°/−45°]s), and M3 ([0°/45°/90°/−45°]s) (Table 1). Composites were produced in dimensions of $500 \times 300 \times 6$ mm and their technical properties are given in Table 2. The materials were produced by the vacuum bagging method for a lighter, stronger, and more stable structure.

Fig. 1 Flowchart of experimental and statistical procedures

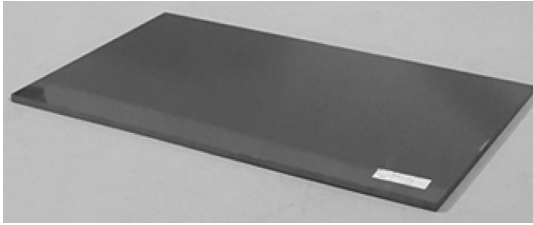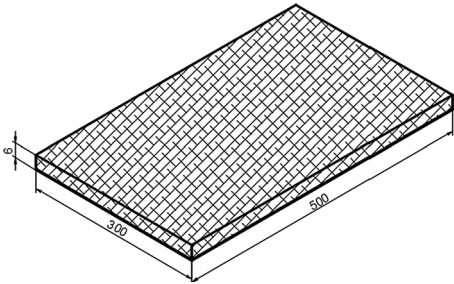**Table 1** Codes for CFRP composites and their fiber orientation angles [50]

Number	CFRP composite	Fiber orientation angle	Fiber orientation angles of CFRP composites
1	M1	$[0°/90°]_s$	
2	M2	$[+45°/−45°]_s$	
3	M3	$[0°/45°/90°/−45°]_s$	

M1 $[0°/90°]_s$ M2 $[+45°/-45°]_s$ M3 $[0°/45°/90°/-45°]_s$

Table 2 Technical properties of CFRP composite materials [50]

Weaving type	Twill 2×2
Fabric weight	200 g/m^2
Fiber volume ratio	50%
Number of layers	24
Thickness of each layer	~ 0.2 to 0.5 mm
Resin type	Epoxy
Number of filaments	3 K
Production method	Vacuum bagging

2.2 AWJ drilling experiments

Drilling operations were carried out on the CFRP composites using a Bystronic Byjet Flex 8030 3-axis AWJ machine with a maximum water pressure of 5300 bar. In order to prevent the garnet abrasive accumulated in the mixing tube from damaging the material between drilling processes, the drilling was carried out with a delay of 3 s. In addition, the aim was to minimize hole damage by starting the hole drilling process from the center of the hole (Fig. 2) [50].

2.3 Drilling parameters and experimental design method

Water pressure (*WP*), nozzle approach distance (*L*), nozzle feed rate (*F*), and hole diameter (*D*) were chosen as the process parameters for the AWJ drilling of the CFRP composites. The levels of the process parameters are given in Table 3. Abrasive flow rate (350 g/min), nozzle diameter (0.80 mm), and 80-mesh garnet (34–40% SiO_2, 31–34% Fe_2O_3, 18–20% Al_2O_3, 6–7% MgO, 2% CaO, 0.5–1.0%
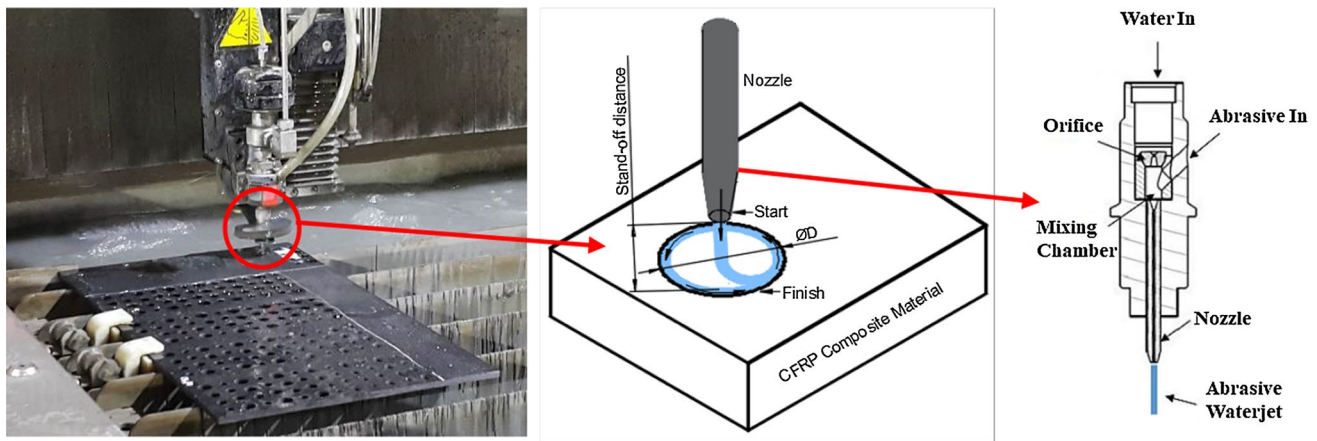
Fig. 2 AWJ drilling of CFRP composite [50]

Table 3 AWJ drilling parameters and their levels

Symbol	Parameters (units)	Level 1	Level 2	Level 3	Level 4
WP	Water pressure (bar)	3600	4300	4800	5300
F	Traverse feed rate (mm/min)	750	1500	2000	3000
L	Stand-off distance (mm)	1	2	3	4
D	Hole diameter (mm)	8	10	12	14

MnO, 1–2% TiO_2 and < 1% SiO_2) abrasive type were kept constant throughout the machinability experiments [50]. The Taguchi method was used because it reduced the costs of the experimental study and provided a systematic approach for determining the optimum AWJ process parameters and investigating the effects of the specified drilling parameters on D_f and R_a. The L_{16} (4^4) orthogonal array was chosen as the most suitable for the experimental design [50].

In this study, the "Smaller is better" approach was chosen to calculate the appropriate signal/noise (*S/N*) ratio for obtaining the lowest D_f and the lowest R_a (Eq. 1) [41, 42, 48–50].

$$S/N = -10 \log \left[\sum_{i=1}^{n} yi^2 \right] \tag{1}$$

After the AWJ drilling of the CFRP composites, ANOVA was applied to determine the degree of influence of the processing parameters on the quality characteristics [49, 50]. The ANOVA was performed at 5% significance level and 95% reliability level [49, 50]. The Taguchi method evaluations and ANOVA analyses were carried out using the Minitab 17 package program. The optimal levels of the control factors with significant effects from the ANOVA table, the predictive optimal quality characteristics ($D_{f\_}$opt), and the predictive optimal average surface roughness ($R_{a\_}$opt) were determined. The confidence interval (CI) was calculated to determine the quality characteristics of the validation experiments. The CI predictive optimal quality characteristics were calculated for $D_{f\_}$opt and $R_{a\_}$opt using Eq. (2) [50].

$$CI = \sqrt{F_{\alpha:1,V2} \cdot V_e \cdot \left(\frac{1}{n_{eff}} + \frac{1}{r} \right)} \tag{2}$$

Here, $F_{\alpha:1,V2}$ represents the *F*-ratio of significance level α, α is the significance level, V_2 is the degree of freedom for combined error variance, V_e is the combined error variance, r is the number of repeated experiments, and n_{eff} is the number of valid measurement results. The number of valid measurement results (n_{eff}) is calculated using Eq. (3) [50].

$$n_{eff} = \frac{T_{exp}}{1 + dof} \tag{3}$$

Here, T_{exp} is the total number of experiments and dof is the total degree of freedom factors used for prediction [50].

2.4 Surface roughness, delamination measurement, and calculation of delamination factor

Surface roughness is one of the most important parameters in the machining process. Hole surface quality will strongly affect manufactured parts throughout their service life, especially for components that come into contact with other elements or materials. Poor hole surface also affects the fatigue

life of the hole [24]. In this study, the average surface roughness value (R_a) was used to characterize the surface quality of the hole. R_a is the arithmetic mean of all values related to deviations from the profile mean line along the roughness profile. After the drilling tests, the average surface roughness measurements were carried out in accordance with the ISO 4287 standard. Regions where the average surface roughness measurement was taken are shown in Fig. 3a. For each hole, four measurements were made using the Mitutoyo SJ-410 roughness measuring device (Fig. 3a) and the average surface roughness values were determined for each hole by taking the arithmetic average of the values obtained from the four different regions.

The delamination factor (D_f) was specified as the ratio between the largest diameter (D_{max}) around the hole and the hole diameter (D_o) as shown in Eq. (4) (Fig. 3b) [28].

$$D_f = \frac{D_{max}}{D_0} \tag{4}$$

Microstructure images of the holes were taken with a Nikon ShuttlePix microscope which can provide $20\times - 400\times$

magnification to reveal any delamination formation that had occurred in the material after drilling the CFRP composites via AWJ (Fig. 3c) [36]. Since the amount of damage caused by the abrasive water jet can be different at the entry and the exit of the hole, the images were taken from two different sites: at the hole entry (upper surface) and hole exit (bottom surface).

3 Results and discussion

3.1 Evaluation of experimental delamination factor and surface roughness results

The delamination factor for the hole entry surface (D_{f_u}) and hole exit surface (D_{f_b}) and the arithmetic mean of R_a surface roughness of the hole surfaces obtained in AWJ drilling of M1, M2, and M3 CFRP composites are presented in Table 4. The arithmetic means of D_f and R_a measurements for the CFRP materials were used to draw the plots and to evaluate the effects of the process parameters. In this study, the effects, sequence, effects %, and optimum levels of
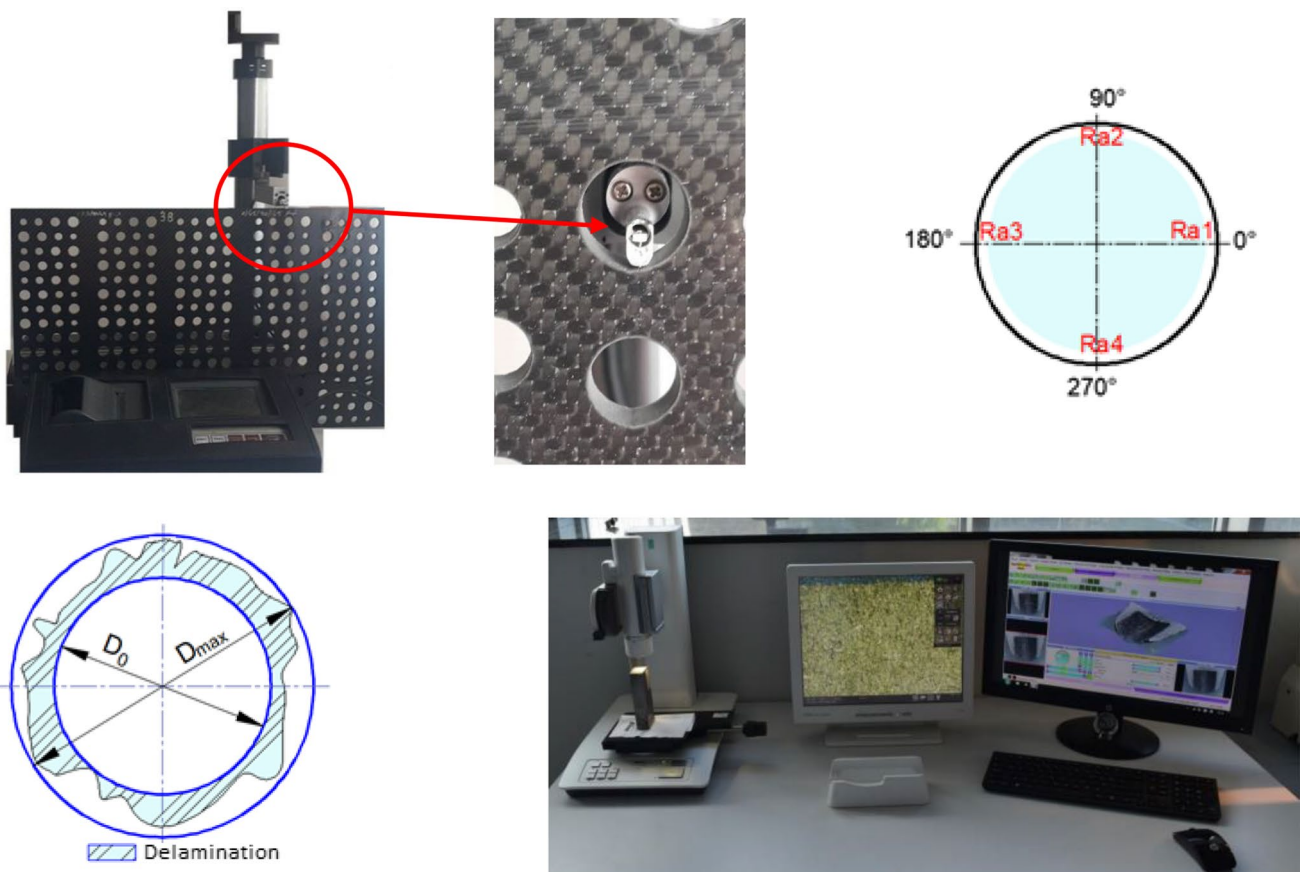
Fig. 3 Delamination factor and surface roughness measurements: **a** measurement of surface roughness, **b** schematic representation of delamination, **c** measurement of delamination formation

Table 4 Experimental design according to the L_{16} orthogonal array, mean, and S/N ratios for delamination factor and surface roughness

Trial number	AWJ drilling parameters and their levels				Mean for delamination factor and average surface roughness									S/N ratio for delamination factor and average surface roughness								
					D_f						R_a (µm)			D_f_S/N (dbA)						R_a_S/N (dbA)		
	WP	F	L	D	M1		M2		M3		M1	M2	M3	M1		M2		M3		M1	M2	M3
	Water pressure	Traverse feed rate	Stand-off distance	Hole diameter	D_f_u	D_f_b	D_f_u	D_f_b	D_f_u	D_f_b				D_f_u	D_f_b	D_f_u	D_f_b	D_f_u	D_f_b			
1	3600	750	1	8	1.245	1.146	1.283	1.148	1.170	1.145	2.080	2.153	1.758	−1.90	−1.18	−2.16	−1.20	−1.36	−1.18	−6.36	−6.66	−4.90
2	3600	1500	2	10	1.247	1.162	1.294	1.157	1.184	1.163	2.163	2.188	2.400	−1.92	−1.30	−2.24	−1.27	−1.47	−1.31	−6.70	−6.80	−7.60
3	3600	2000	3	12	1.264	1.223	1.431	1.315	1.206	1.230	2.441	2.598	2.423	−2.03	−1.75	−3.11	−2.38	−1.63	−1.80	−7.75	−8.29	−7.69
4	3600	3000	4	14	1.383	1.241	1.572	1.380	1.306	1.243	2.606	2.708	2.617	−2.82	−1.88	−3.93	−2.80	−2.32	−1.89	−8.32	−8.65	−8.36
5	4300	750	2	12	1.203	1.125	1.258	1.126	1.165	1.136	1.863	1.746	1.543	−1.61	−1.02	−1.99	−1.03	−1.33	−1.11	−5.40	−4.84	−3.77
6	4300	1500	1	14	1.193	1.124	1.219	1.114	1.157	1.128	1.788	1.678	1.468	−1.53	−1.02	−1.72	−0.94	−1.27	−1.05	−5.05	−4.50	−3.33
7	4300	2000	4	8	1.219	1.142	1.269	1.143	1.166	1.139	2.063	1.950	1.703	−1.72	−1.15	−2.07	−1.16	−1.33	−1.13	−6.29	−5.80	−4.62
8	4300	3000	3	10	1.209	1.135	1.264	1.133	1.165	1.137	1.966	1.838	1.637	−1.65	−1.10	−2.03	−1.08	−1.33	−1.12	−5.87	−5.29	−4.28
9	4800	750	3	14	1.142	1.099	1.203	1.097	1.123	1.106	1.658	1.508	1.205	−1.15	−0.82	−1.61	−0.80	−1.01	−0.88	−4.39	−3.57	−1.62
10	4800	1500	4	12	1.166	1.120	1.204	1.105	1.140	1.107	1.675	1.563	1.413	−1.33	−0.98	−1.61	−0.87	−1.14	−0.88	−4.48	−3.88	−3.00
11	4800	2000	1	10	1.116	1.081	1.167	1.080	1.096	1.076	1.200	1.238	0.998	−0.95	−0.68	−1.34	−0.67	−0.80	−0.64	−1.58	−1.85	0.02
12	4800	3000	2	8	1.137	1.097	1.192	1.091	1.114	1.080	1.445	1.473	1.090	−1.12	−0.80	−1.53	−0.76	−0.94	−0.67	−3.20	−3.36	−0.75
13	5300	750	4	10	1.107	1.081	1.138	1.068	1.085	1.075	1.265	1.368	1.003	−0.88	−0.68	−1.12	−0.57	−0.71	−0.63	−2.04	−2.72	−0.03
14	5300	1500	3	8	1.132	1.088	1.171	1.084	1.101	1.080	1.353	1.385	1.018	−1.08	−0.73	−1.37	−0.70	−0.84	−0.67	−2.63	−2.83	−0.15
15	5300	2000	2	14	1.105	1.075	1.133	1.037	1.081	1.069	1.058	1.080	0.948	−0.87	−0.63	−1.08	−0.32	−0.68	−0.58	−0.49	−0.67	0.46
16	5300	3000	1	12	1.091	1.055	1.130	1.029	1.080	1.058	1.013	0.990	0.920	−0.76	−0.47	−1.06	−0.25	−0.67	−0.49	−0.11	0.09	0.72
Maximum					1.383	1.241	1.572	1.380	1.306	1.380	2.606	2.708	2.617									
Minimum					1.091	1.055	1.130	1.029	1.080	1.029	1.013	0.990	0.920									
Mean					1.185	1.125	1.246	1.132	1.146	1.123	1.727	1.717	1.509									
Mean					1.160						1.622											
Hole entry and exit delamination factor % difference					5.33%		10.07%		2.04%		−	−	−	−	−							

drilling parameters of AWJ-drilled M1, M2, and M3 CFRP composites were determined by the Taguchi method [50]. The Taguchi method reduces experimental costs by reducing the number of experiments and uses a systematic approach to enable successful performance of optimization operations [50]. The delamination factor and surface roughness values were converted to S/N ratios according to the "Smaller is better" approach using Eq. (1) to perform statistical analyses according to the Taguchi method (Table 4). The signal value represents the actual value given by the system and is intended to be measured, while the noise factor represents the share of undesired factors within the measured value. The S/N ratio analysis gave important information about the delamination factor and the nature of R_a surface roughness values measured in the drilling of the M1, M2, and M3 CFRP composites under the specified AWJ drilling parameters [50].

The material with the greatest difference in delamination formation between the hole entry and hole exit was the

M2 CFRP with a fiber orientation ratio of $[+45°/−45°]$ s. A delamination factor difference of 10.07% was calculated between the hole entry and hole exit. The difference between the hole entry and hole exit delamination factor for the M1 and M3 CFRP composites was 5.33% and 2.04%, respectively (Table 4). When evaluated in terms of surface quality, R_a surface roughness values in the range of 2.708−0.990 µm were obtained when drilling the M2 CFRP composite at different process parameter levels. The mean of the delamination factor and R_a surface roughness was 1.160 and 1.622 µm, respectively. In the study conducted by Unde et al. [18], the delamination factor and R_a value were approximately 2.239 and 6.967 µm, respectively, in the AWJ machining of CFRP laminate with a fiber orientation angle of 45°. The delamination factor and R_a surface roughness values obtained in this study seem to be quite satisfactory.

In Fig. 4, the delamination factor and R_a surface roughness values obtained as a result of AWJ drilling experiments performed at different levels of control factors according to
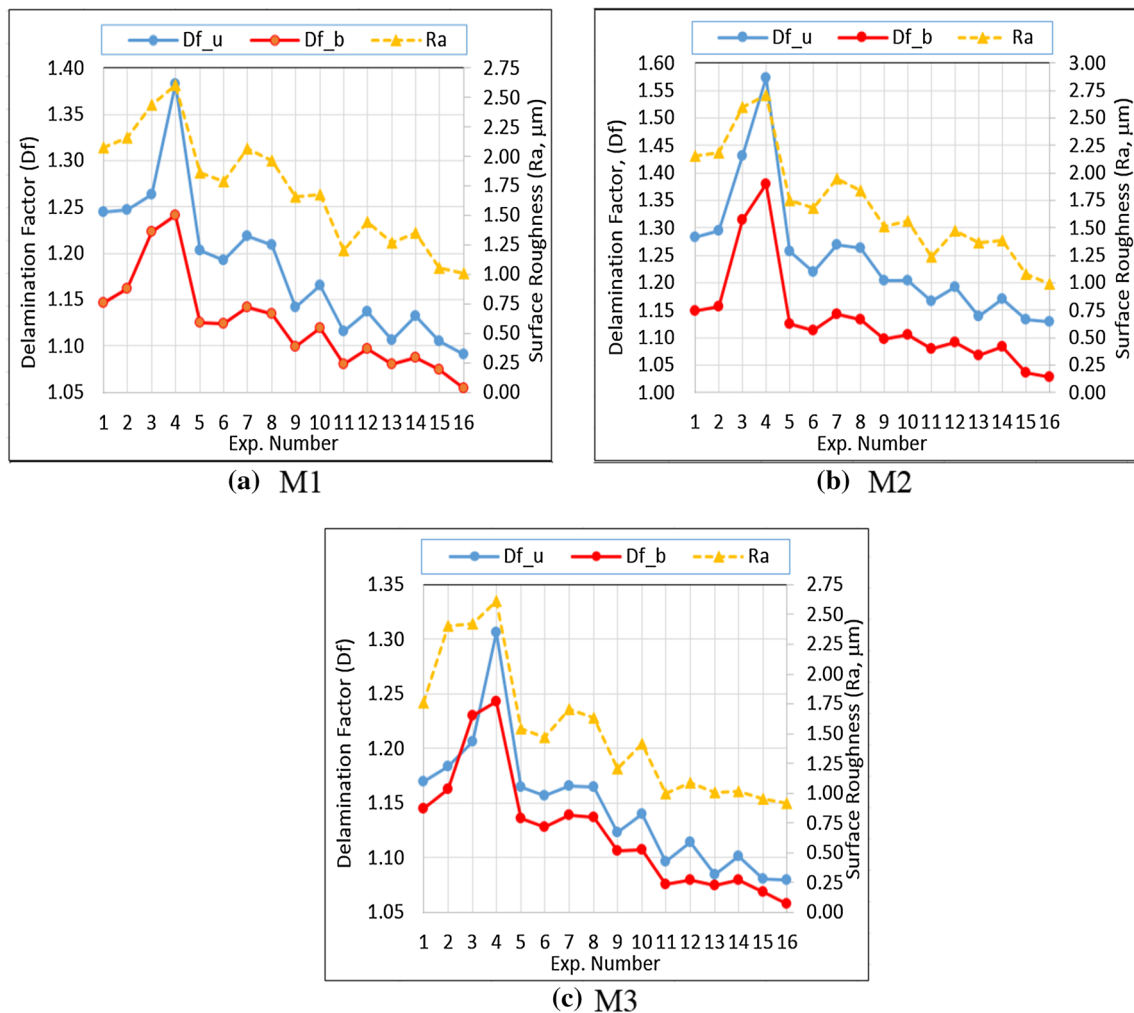

(a) M1

(b) M2

(c) M3

Fig. 4 Delamination factor (D_f_u and D_f_b) and surface roughness (R_a) values for M1, M2, and M3 CFRPs in the order of the experiments

the Taguchi method L_{16} orthogonal array are shown in the order of the experiments. As can be seen in Fig. 4, in this study, the highest delamination factor and R_a surface roughness values were obtained in the AWJ drilling of all three composite (M1, M2, and M3 CFRP) materials under test conditions of Experiment No. 4 ($P = 3600$ bar, $F = 3000$ mm/min, $L = 4$ mm, and $D = 14$ mm), while the lowest delamination factor and R_a surface roughness values were obtained under test conditions of Experiment No. 16 ($P = 5300$ bar, $F = 3000$ mm/min, $L = 1$ mm, and $D = 12$ mm). However, based on these results (Fig. 4), it is not possible to say that the conditions of Experiment 16 are the optimum levels of drilling parameters to obtain a minimum delamination factor and minimum R_a surface roughness values in the AWJ drilling of CFRP composites with three different fiber orientation angles, nor is it possible to say from Fig. 4a–c that the angle of fiber orientation does not have a significant effect on the delamination factor and surface roughness. The surface roughness values fluctuated when machining CFRPs with different fiber orientation angles [40]. Therefore, an evaluation of Experiment 16 test results was carried out using the Taguchi method.

3.2 Effects of fiber orientation angle differences on delamination factor and surface roughness

The delamination factor and R_a surface roughness depending on the fiber orientation angle difference are presented in Fig. 5. The highest delamination factor and R_a surface roughness values were obtained in the drilling of M2 CFRP composites with [+45°/− 45°]s fiber orientation, whereas the lowest delamination factor and R_a surface roughness values were obtained in the drilling of M3 CFRP composites with[0°/45°/90°/− 45°]s fiber orientation. Again, a lower delamination factor and R_a surface roughness values were obtained when drilling the M1 CFRP with [0°/90°]s fiber
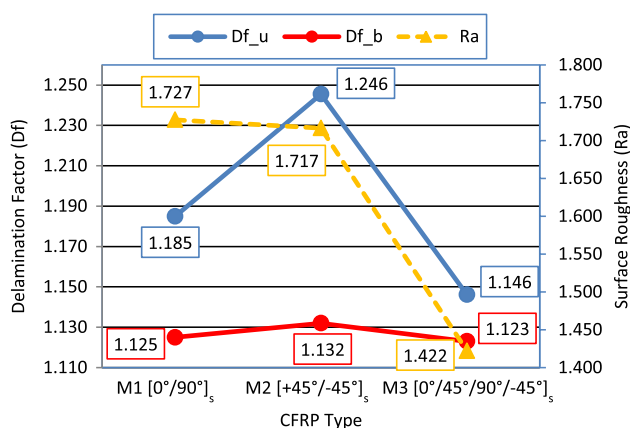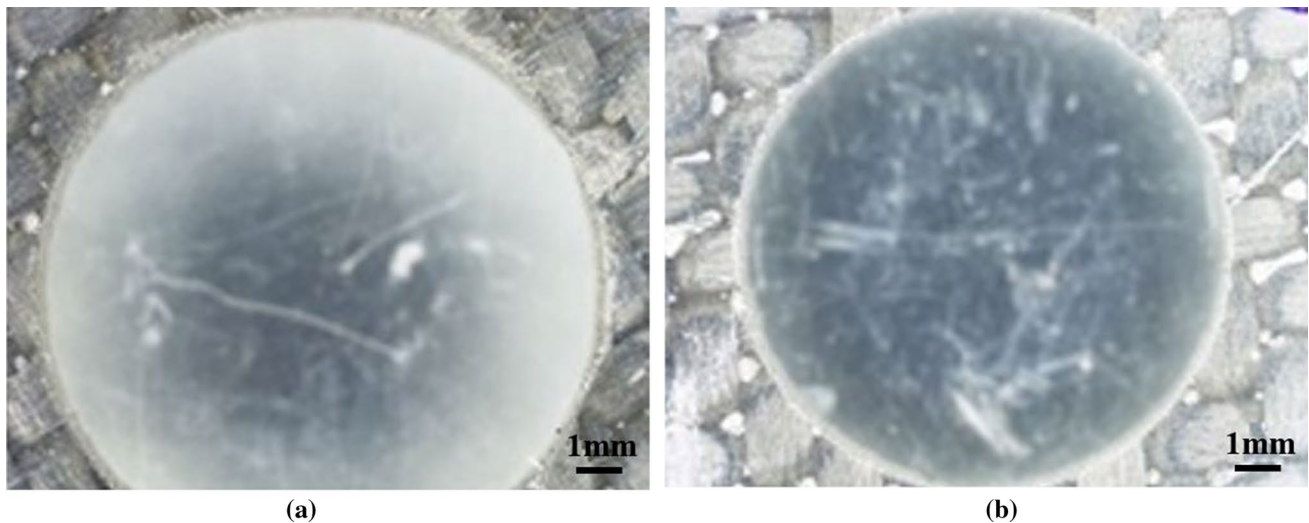
orientation. In the study conducted by Unde et al., the delamination factor and surface roughness values were higher in the AWJ machining of CFRPs with a 45° fiber orientation angle compared to the CFRPs with a 90° fiber orientation angle. The cutting plane is elliptical for a 45° fiber orientation angle and circular for 90°. Sharper and cleaner cuts are possible when cutting CFRPs with a 90° fiber orientation angle. This has been attributed to the greater resistance offered by the fibers in 45° orientation. Greater resistance can result from the large cutting area at 45° compared to 90°. In 45° fiber orientations, the cutting plane area is greater compared to that of 90° due to the reduction in cutting angle. As the cutting angle decreases, the cutting plane becomes more elliptical, resulting in an increase in the area to be cut. In this context, the findings of this study are similar to those of Unde et al. [18]. Figure 5 shows that for all (M1, M2, and M3) CFRP composites, there are more delamination formations at the hole entry than at the hole exit in average.

3.3 Delamination factor

In the drilling of CFRP composites, damage such as surface chipping or edge deformation, delamination, and internal cracking occur on the upper surface of the hole [34, 35]. Delamination is the main defect in the machining of composite materials [18, 26–29, 36, 38, 41, 43].

3.3.1 Evaluation of delamination formation

In this study, quantitative evaluations were performed for the delamination factor (using Eq. 4), which is the degree of delamination damage at the hole entry (top surface of the CFRPs) and hole exit (bottom surface of the CFRPs). Delamination was observed on both sides of the M1, M2, and M3 CFRP composites, namely the top (hole entry) and bottom (hole exit) [31, 36]. Delamination formations in the form of outward peeling were observed at the hole entry and hole exit in all of the CFRP composites drilled using AWJ (Fig. 6a, b) [28]. When AWJ drilling the CFRP composites with three different fiber orientations, greater delamination occurred on the surface at the hole entry than at the hole exit (Table 4, Fig. 4). It has been reported that delamination is initiated by the shock wave produced by the jet in AWJ machining [18, 23, 27, 29, 34, 36] at the first cutting stage when the jet surface touches the material surface [27, 29, 34, 36]. The crack points that are initiated by the shock wave pulse then spread to the ends that support the water wedge and abrasive embedding results from the jet slurry penetration [23, 27]. Therefore, delamination is higher at the upper surface (hole entry) than at the bottom surface (hole exit) [34, 43] because there is more peeling and layering at the upper part than at the bottom. When the abrasive particles reach the upper surface, they have more energy to cut the

Fig. 5 Delamination factor (D_f_u, D_f_b) and surface roughness (R_a) values depending on fiber orientation

(a)   **(b)**

Fig. 6 Maximum and minimum deformation in the form of peeling at the hole entry in AWJ drilling of the M1 CFRP composite: **a** $D_f = 1.383$, Exp. No. 4, **b** $D_f = 1.091$, Exp. No. 16

material, and then the particles continuously lose energy during the spread of the jet [18, 43].

3.3.2 Main effects of AWJ process parameters on delamination factor

The *S/N* ratios for D_f values and the D_f values calculated in Table 4 have been converted into response tables (Table 5). The effect size for each process parameter can be determined through the rank line of the response table. Higher or lower differences between the highest and lowest *S/N* ratio values calculated at different levels of each of the process parameters were used to identify the effective parameters on the delamination factor and to determine the order of action of these parameters [50]. As Table 5 clearly shows, the most effective parameter on D_f is water pressure. The effect order of the process parameters on D_f in the AWJ drilling of CFRP composites M1 and M3 was water pressure, stand-off distance, hole diameter, and traverse feed rate (Table 5a, b, e, f). For the M2 CFRP composites, this order was water pressure, stand-off distance, traverse feed rate, and hole diameter (Table 5c, f). The optimum AWJ drilling parameters levels for the minimum delamination factor in the AWJ drilling of CFRP with three different fiber orientation angles was identified as $WP_4–F_1–L_1–D_2$. In Table 6a–f, optimum levels of AWJ drilling parameters are marked with "a". The optimum levels of AWJ drilling parameters were determined as $P = 5300$ bar, $F = 750$ mm/min, $L = 1$ mm, and $D = 10$ mm, via Table 2.

The main effect plots indicating the effects of AWJ drilling parameters on the delamination factor are presented in Fig. 7 with the *S/N* ratios. Figure 7 shows the effect order of each process parameters and the differing delamination

factors depending on the different levels of the process parameters. Figure 7 shows that delamination formation was higher in the hole entry (upper surface of the workpiece) than the hole exit (bottom surface of the workpiece) for all (M1, M2, and M3) CFRP composites. Therefore, the calculated delamination factors are higher. The AWJ drilling parameters had the same order of effect on the delamination factor for the M1 and M2 CFRP composites (water pressure, stand-off distance, traverse feed rate, and hole diameter, respectively). The effect order of the control factors in Fig. 7 is the same as in Table 5.

Due to the increase in water pressure, the formation of delamination (thus, the delamination factor) at the hole entry and hole exit decreased [35] (Fig. 7a–c). This was attributed to faster cutting of the composite materials with increased water pressure, which caused the kinetic energy of the abrasive jet to increase [18, 24, 25, 31, 32, 36]. As seen in Fig. 7a–c, with the increase in traverse feed rate, the delamination factor also increased slowly [31, 32, 37]. This delamination was formed because the jet trying to wear and cut the workpiece during the circular drilling movement had a higher feed rate, so the field had less impact on the contact surface at the time of cutting, and this short time was not sufficient to cut the part more smoothly and closer to the shape. When the traverse feed rate is high, all the fiber particles forming the composite cannot be cut, and consequently, delamination occurs with the traverse motion. In summary, the traverse feed rate decides the interruption time during the AWJ process [18].

In addition, the delamination increases with an increase in the traverse feed rate due to the impact of fewer abrasive particles in a short time and with less overlap of the machining effect [32]. The stand-off distance has been found to

Table 5 Response table for delamination factor means and signal-to-noise (*S/N*) ratios

S/N ratios for D_f_u (dB)					Means for D_f_u				
Level	A (*WP*)	B (*F*)	C (*L*)	D (*D*)	Level	A (*WP*)	B (*F*)	C (*L*)	D (*D*)
(a) M1 CFRP (delamination factor for hole entry)									
1	− 2.1680	− 1.3862	− 1.2865	− 1.4539	1	1.285	1.174[a]	1.161[a]	1.183
2	− 1.6267	− 1.4653	− 1.3763	− 1.3505	2	1.206	1.185	1.173	1.170[a]
3	− 1.1389	− 1.3939	− 1.4784	− 1.4327	3	1.140	1.176	1.187	1.181
4	− 0.8959	− 1.5842	− 1.6884	− 1.5925	4	1.109[a]	1.205	1.219	1.206
Difference	1.2721	0.1979	0.4019	0.2419	Difference	0.176	0.031	0.057	0.036
Rank	1	4	2	3	Rank	1	4	2	3
S/N ratios for D_f_b (dB)					**Means for D_f_b**				
Level	A (*WP*)	B (*F*)	C (*L*)	D (*D*)	Level	A (*WP*)	B (*F*)	C (*L*)	D (*D*)
(b) M1 CFRP (Delamination factor for hole exit)									
1	− 1.5279	− 0.9258	− 0.8351	− 0.9684	1	1.193	1.113[a]	1.101[a]	1.118
2	− 1.0729	− 1.0091	− 0.9399	− 0.9393	2	1.132	1.123	1.115	1.115[a]
3	− 0.8212	− 1.0516	− 1.1002	− 1.0552	3	1.099	1.130	1.136	1.131
4	− 0.6256	− 1.0611	− 1.1724	− 1.0847	4	1.075[a]	1.132	1.146	1.135
Difference	0.9024	0.1353	0.3373	0.1455	Difference	0.118	0.019	0.044	0.020
Rank	1	4	2	3	Rank	1	4	2	3
S/N ratios for D_f_u (dB)					**Means for D_f_u**				
Level	A (*WP*)	B (*F*)	C (*L*)	D (*D*)	Level	A (*WP*)	B (*F*)	C (*L*)	D (*D*)
(c) M2 CFRP (Delamination factor for hole entry)									
1	− 2.861	− 1.722	− 1.572	− 1.783	1	1.395	1.220[a]	1.200[a]	1.229
2	− 1.954	− 1.736	− 1.711	− 1.684	2	1.253	1.222	1.219	1.216[a]
3	− 1.521	− 1.902	− 2.031	− 1.945	3	1.192	1.250	1.267	1.256
4	− 1.160	− 2.138	− 2.183	− 2.085	4	1.143[a]	1.290	1.296	1.282
Difference	1.701	0.416	0.612	0.400	Difference	0.252	0.069	0.096	0.066
Rank	1	3	2	4	Rank	1	3	2	4
S/N ratios for D_f_b (dB)					**Means for D_f_b**				
Level	A (*WP*)	B (*F*)	C (*L*)	D (*D*)	Level	A (*WP*)	B (*F*)	C (*L*)	D (*D*)
(d) M2 CFRP (Delamination factor for hole exit)									
1	− 1.9104	− 0.9013	− 0.7633	− 0.9542	1	1.250	1.110[a]	1.093[a]	1.116
2	− 1.0535	− 0.9431	− 0.8424	− 0.8978	2	1.129	1.115	1.103	1.110[a]
3	− 0.7741	− 1.1309	− 1.2420	− 1.1312	3	1.093	1.144	1.157	1.144
4	− 0.4590	− 1.2217	− 1.3493	− 1.2137	4	1.055[a]	1.158	1.174	1.157
Difference	1.4514	0.3205	0.5860	0.3160	Difference	0.196	0.048	0.081	0.047
Rank	1	3	2	4	Rank	1	3	2	4
S/N ratios for D_f_u (dB)					**Means for D_f_u**				
Level	A (*WP*)	B (*F*)	C (*L*)	D (*D*)	Level	A (*WP*)	B (*F*)	C (*L*)	D (*D*)
(e) M3 CFRP (Delamination factor for hole entry)									
1	− 1.6941	− 1.1016	− 1.0238	− 1.1178	1	1.216	1.136[a]	1.126[a]	1.138
2	− 1.3134	− 1.1769	− 1.1019	− 1.0746	2	1.163	1.146	1.136	1.133[a]
3	− 0.9699	− 1.1084	− 1.1992	− 1.1900	3	1.118	1.137	1.149	1.148
4	− 0.7223	− 1.3129	− 1.3749	− 1.3174	4	1.087[a]	1.166	1.174	1.167
Difference	0.9718	0.2113	0.3511	0.2428	Difference	0.130	0.030	0.048	0.034
Rank	1	4	2	3	Rank	1	4	2	3

Table 5 (continued)

S/N ratios for D_f_b (dB)					Means for D_f_b				
Level	A (WP)	B (F)	C (L)	D (D)	Level	A (WP)	B (F)	C (L)	D (D)
(f) M3 CFRP (Delamination factor for hole exit)									
1	− 1.5438	− 0.9467	− 0.8371	− 0.9109	1	1.195	1.115[a]	1.102[a]	1.113
2	− 1.0999	− 0.9773	− 0.9168	− 0.9228	2	1.135	1.119	1.112	1.111[a]
3	− 0.7657	− 1.0361	− 1.1142	− 1.0696	3	1.092	1.128	1.138	1.133
4	− 0.5915	− 1.0407	− 1.1328	− 1.0976	4	1.071[a]	1.129	1.141	1.137
Difference	0.9523	0.0940	0.2957	0.1867	Difference	0.125	0.014	0.039	0.026
Rank	1	4	2	3	Rank	1	4	2	3

[a]Optimum level

significantly affect delamination at both the upper and bottom surface of the CFRP laminate [18]. Delamination and fiber withdrawal were also prominent in the AWJ machining of carbon epoxy composites processed at low water pressure and high traverse feed rate [31, 32]. A lower delamination factor was obtained at a lower stand-off distance [37] (Fig. 7a–c). The low stand-off distance means that the nozzle is closer to the workpiece surface when drilling with AWJ, and thus, the jet's kinetic energy trying to pierce the workpiece will not decrease and its ability to cut will increase. In addition, the diameter of the water jet coming out of the nozzle will increase with increased stand-off distance, so the direction and flow pattern of the abrasive grains in the water will change, and the water jet cutting ability will decrease. In this case, delamination formation will increase and the desired clean cut in the workpiece will not be achieved. In other words, the stand-off distance determines the cutting area, which increases or decreases the impact area. As the stand-off distance increases, the jet is deflected and the cutting area increases with the increase of deviations in the jet [18]. Phapale et al. [24] stated that a high stand-off distance caused the jet to deflect before collision. As can be seen in Fig. 7a–c, although the hole diameter did not have a significant stable effect on the delamination factor, the delamination factor increased with increasing hole diameter. This was due to the reduction in the hole radius for lower hole diameters at a constant feed rate. In a smaller diameter hole compared to a large diameter hole, the water jet will act on the same or close surfaces in more time and thus, the hole is formed closer to the net shape and the fibers are cut more easily.

3.3.3 Analysis of variance (ANOVA) for delamination factor

ANOVA was performed to determine the effects of process parameters on the selected performance/quality characteristics for each experiment in the L_{16} orthogonal array with a 95% confidence interval. The ANOVA results for hole entry surface delamination factor (D_f_u) and hole exit surface delamination factor (D_f_b) in the AWJ drilling of the M1, M2, and M3 CFRPs are presented in Table 6. The results obtained from this ANOVA table are as follows:
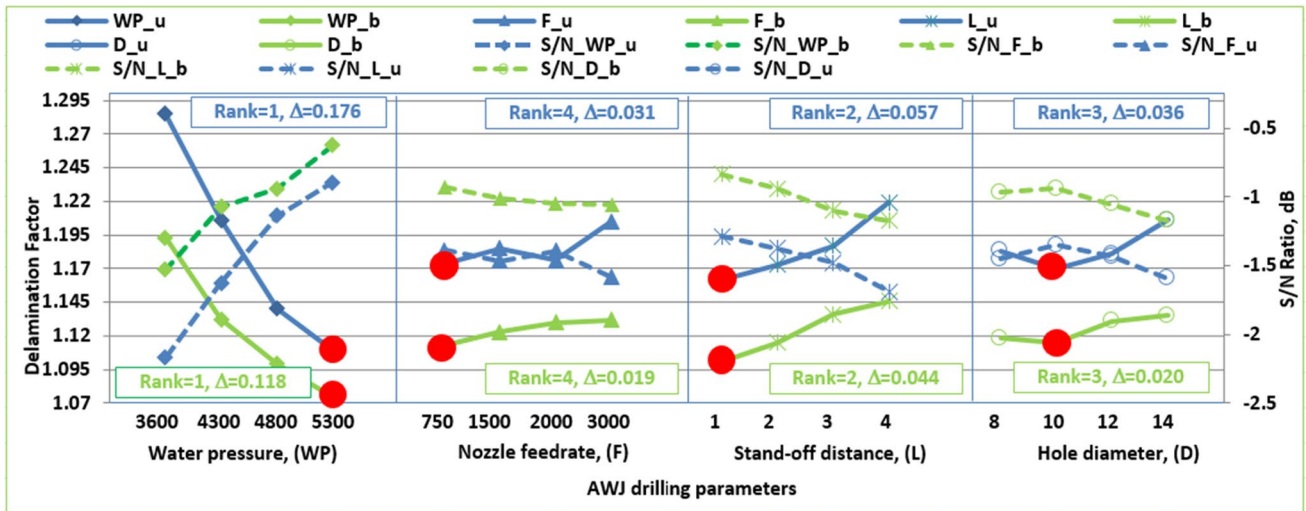
- The most effective parameters on hole entry and hole exit delamination factor in terms of % contribution in drilling the M1 CFRP composite were water pressure (82.4% and 79.8%) and stand-off distance (8.4% and 12.4%). The effect of the other drilling parameters remained below 5%. However, the effect of stand-off distance was not statistically significant (Since $P > 0.05$). The correlation coefficient (R^2) of the ANOVA for the hole entry and hole exit delamination factors was calculated as 96.5% and 97.3%, respectively (Table 6a).

- In the drilling of the M2 CFRP composite, the most effective parameters on the hole entry and hole exit delamination factors were water pressure (70.9% and 66.6%) and stand-off distance (11.4% and 14.9%) in terms of % contribution. The effect of other drilling parameters remained below 7%. However, the effect of stand-off distance was not statistically significant (Since $P > 0.05$). The correlation coefficient (R^2) of the ANOVA for the hole entry and hole exit delamination factors was calculated as 93.6% and 91.2%, respectively (Table 6b).

- In similar trends, the most effective parameters on the hole entry and hole exit delamination factors in the drilling of the M3 CFRP composite were water pressure (75.1% and 81.5%) and stand-off distance (10.3% and 10.2%) in terms of % contribution. However, the effect of stand-off distance was not statistically significant (Since $P > 0.05$). The effect of other drilling parameters remained below 6%. The correlation coefficient (R^2) of the ANOVA for the hole entry and hole exit delamination factors was calculated as 95.44%, and 97.7%, respectively (Table 6c).

In the study conducted by Phapale et al. [24], water pressure and stand-off distance played a more dominant role on the delamination formation of CFRP composites compared

Table 6 Analysis of variance for delamination factor of upper and bottom surfaces

D_{f_u}

Source	Degree of freedom	Sum of square	Mean square	F-ratio	Prob. > F	Contribution %
(a) M1 CFRP						
A (WP)	3	0.072831	0.024277	23.76	0.014[a]	82.4
B (F)	3	0.002387	0.000796	0.78	0.579	2.7
C (L)	3	0.007401	0.002467	2.41	0.244	8.4
D (D)	3	0.002729	0.000910	0.89	0.537	3.1
Error	3	0.003066	0.001022			3.5
Total	15	0.088413				100.0
$S=0.03197$, RSD$=0.0319$, $R^2=96.5\%$, $R^2(\text{adj})=82.7\%$						
(b) M2 CFRP						
A (WP)	3	0.14329	0.047762	11.11	0.039[a]	70.9
B (F)	3	0.01253	0.004178	0.97	0.509	6.2
C (L)	3	0.02312	0.007707	1.79	0.322	11.4
D (D)	3	0.01034	0.003446	0.80	0.570	5.1
Error	3	0.01290	0.004300			6.4
Total	15	0.20218				100.0
$S=0.0655744$, RSD$=0.0655$, $R^2=93.6\%$, $R^2(\text{adj})=68.10\%$						
(c) M3 CFRP						
A (WP)	3	0.038193	0.012731	16.46	0.023[a]	75.1
B (F)	3	0.002367	0.000789	1.02	0.494	4.7
C (L)	3	0.005262	0.001754	2.27	0.259	10.3
D (D)	3	0.002735	0.000912	1.18	0.448	5.4
Error	3	0.002321	0.000774			4.6
Total	15	0.050878				100.0
$S=0.02781$, RSD$=0.0278$, $R^2=95.44\%$, $R^2(\text{adj})77.2\%$						

D_{f_b}

| Source	Degree of freedom	Sum of square	Mean square	F-ratio	Prob. > F	Contribution %
(a) M1 CFRP						
A (WP)	3	0.031415	0.010472	30.06	0.010[a]	79.8
B (F)	3	0.000913	0.000304	0.87	0.543	2.3
C (L)	3	0.004897	0.001632	4.69	0.118	12.4
D (D)	3	0.001113	0.000371	1.06	0.480	2.8
Error	3	0.001045	0.000348			2.7
Total	15	0.039384				100.0
$S=0.01867$, RSD$=0.0186$, $R^2=97.3\%$, $R^2(\text{adj})=86.7\%$						
(b) M2 CFRP						
A (WP)	3	0.085762	0.028587	7.59	0.045[a]	66.6
B (F)	3	0.006443	0.002148	0.57	0.672	5.0
C (L)	3	0.019189	0.006396	1.70	0.337	14.9
D (D)	3	0.006037	0.002012	0.53	0.690	4.7
Error	3	0.011297	0.003766			8.8
Total	15	0.128727				100.0
$S=0.06136$, RSD$=0.0613$, $R^2=91.2\%$, $R^2(\text{adj})=56.1\%$						
(c) M3 CFRP						
A (WP)	3	0.036263	0.012088	35.22	0.008[a]	81.5
B (F)	3	0.000563	0.000188	0.55	0.684	1.3
C (L)	3	0.004516	0.001505	4.39	0.128	10.2
D (D)	3	0.002104	0.000701	4.39	0.128	4.7
Error	3	0.001030	0.000343			2.3
Total	15	0.044475				100.0
$S=0.01852$, RSD$=0.0185$, $R^2=97.7\%$, $R^2(\text{adj})=98.47\%$						

[a] Parameter with statistically significant effect, $P < 0.05$

(a) M1 CFRP
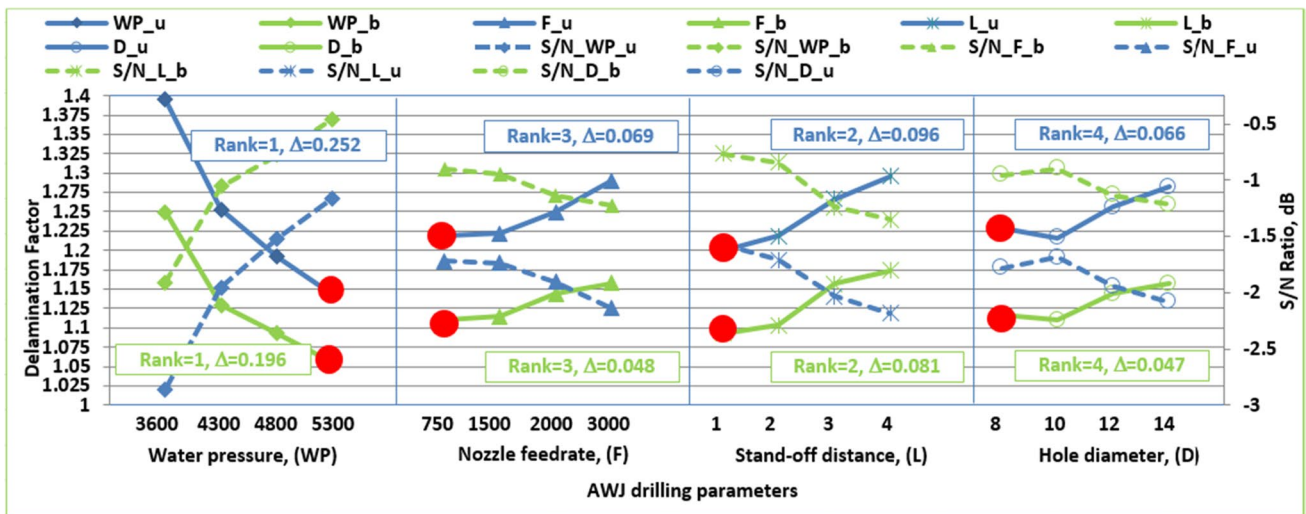
(b) M2 CFRP
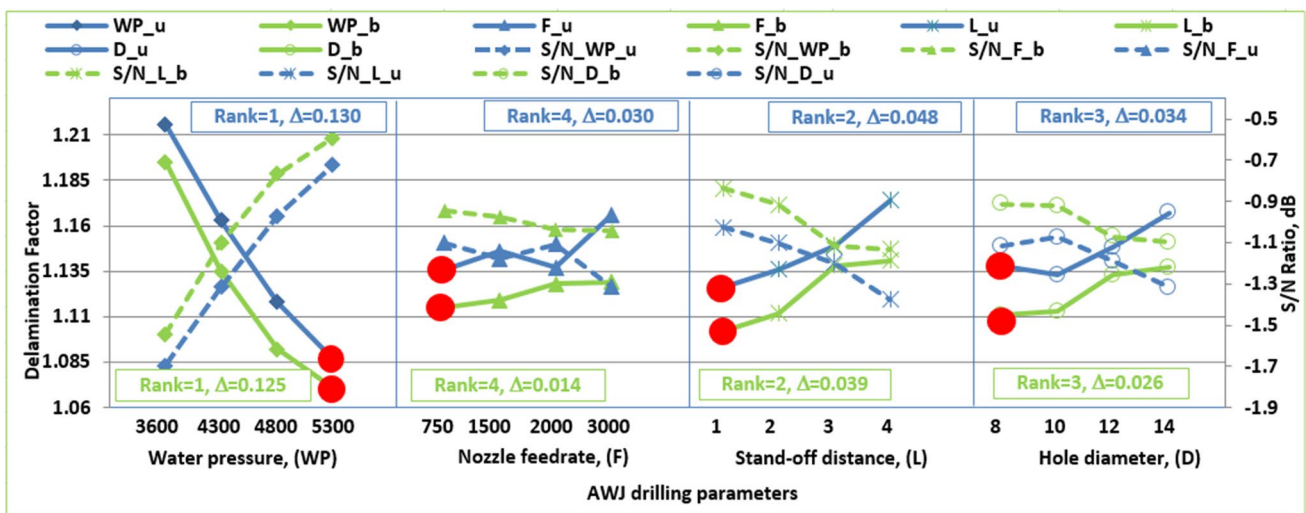
(c) M3 CFRP

Fig. 7 Main effects of AWJ drilling parameters on delamination factor of upper (u-blue) and bottom (b-green) workpiece surfaces (color figure online)

to other process parameters. Although traverse feed rate was the most effective parameter in AWJ machining of GFRP composites, no statistically significant effect of stand-off distance was detected [39]. In AWJ drilling of M1, M2, and M2 CFRP composites, correlation coefficients (R^2, %) for D_f_u and D_f_b were calculated as 96.5%, 97.3%, 93.6%, 91.2%, 95.44% and 97.7%, respectively (Table 6). The high R^2 calculated in the ANOVA indicated that the effects of AWJ drilling parameters on the delamination factor can be explained at a high reliability rate. In addition, Residual Standard Deviation (RSD) was calculated in ANOVA for D_f_u and D_f_b. The Residual Standard Deviation/Error (RSD) is a measure used to assess how well a linear regression model fits the data. RSD is calculated by the square root of the mean square ($\sqrt{\text{Mean Square}}$) of residual error in ANOVA. According to this, RSD for D_f_u and D_f_b were calculated as 0.0319, 0.0186, 0.0656%, 0.0613, 0.0278, and 0.0185, respectively (Table 6). When the RSD is exactly 0 then the model fits the data perfectly. Since the calculated RSD values for D_f_u and D_f_b are very close to 0, the models fit the data perfectly.

3.3.4 Predictive optimum values, confidence intervals, and confirmation tests for delamination factor

Confirmation tests, as the next step of the Taguchi method, are conducted to examine quality characteristics [50]. The model used in the confirmation experiments is defined by the total effect created by the process parameters that have a statistically significant effect. This effect is equal to the sum of the effects of each factor. Optimum levels are evaluated considering error losses [50]. The predictive optimal delamination factor (D_f_opt) was calculated by taking into account the statistically significant factor (WP, $P < 0.05$) in the ANOVA performed for the delamination factor from Table 6 and the optimum level of this control factor from Table 5. The results are presented in Table 7, where D_f_opt values for each composite material (M1, M2, and M3 CFRP) are calculated using Eq. (5).

$$D_{f\_opt} = D_{fm} + \left(WP - D_{fm}\right) \tag{5}$$

Here, D_{fm} is the arithmetic mean of the measurement results for D_f and WP are the values determined by the Taguchi method of the optimum levels of the effective parameters determined from the ANOVA in Table 6, respectively. Using Eq. (5), the D_f_opt= 1.109 for the hole entry delamination factor (D_f_u) using the optimum levels of drilling parameters (WP_4–F_1–L_1–D_2) for the M1 CFRP composite material (Table 7). The predictive optimum delamination factor values for the hole entry and hole exit of each CFRP composite are also presented in Table 7. As the next step of the Taguchi method, confidence intervals

(D_f_CI) for the experimental and the calculated predictive optimum D_f values measured by validation experiments are calculated using Eqs. (2) and (3) (Table 7). As can be seen from Table 7, the confidence intervals for the experimental and predictive optimum D_f values for each CFRP material remained within the lower and upper limits of D_f_CI. It is possible to say that the predictive optimum D_f values calculated with the Taguchi method are more precise than those calculated with Eq. (5) (Table 7).

Each CFRP composite material was subjected to confirmation tests by drilling at the optimal drilling parameter levels determined for them to obtain minimum D_f and under conditions not included in the experimental design in Table 4 (WP_4–F_4–L_1–D_3). For each CFRP's (M1, M2 and M3) D_f_u and D_f_b values, the residuals (relative error) between the D_f values obtained by the experiment performed at optimal levels of the AWJ drilling parameters and the predictive D_f value calculated by the Taguchi method and the % ratio of residuals (% ratio of relative error) were calculated and these are presented in Table 7a–c. The residuals for the D_f_u and D_f_b values of M1, M2, and M3 CFRP was obtained as 0.021, 0.03, 0.019, 0.011, 0.015, and 0.014, respectively. The mean of residuals is 0.018. The relative error % ratio for D_f_u and D_f_b values of M1, M2, and M3 CFRP were obtained as 1.94%, 0.29%, 1.79%, 1.12%, 1.42% and 1.38%, respectively. The mean of % ratio of residuals is 1.32%. Similarly, for each CFRP's (M1, M2 and M3) D_f_u and D_f_b values, the residuals (relative error) between the D_f values obtained by the experiment performed at optimal levels of the AWJ drilling parameters and the D_f value obtained by the confirmation test performed at different levels of the AWJ drilling parameters (WP_4–F_4–L_1–D_3) and the % ratio of residuals (% ratio of relative error) were calculated and these are presented in Table 7a–c. The residuals for the D_f_u and D_f_b values of M1, M2, and M3 CFRP was obtained as 0.011, 0.028, 0.068, 0.049, 0.023, and 0.043, respectively. The mean of residuals is 0.037. The relative error % ratio for D_f_u and D_f_b values of M1, M2, and M3 CFRP were obtained as 1.02%, 2.73%, 6.40%, 5.00%, 2.18%, and 4.24%, respectively. The mean of % ratio of residuals is 3.60%. As a result of the confirmation tests, the minimum D_f values obtained were close to the optimal predictive D_f values obtained at the optimal parameter levels determined by the Taguchi method (Table 7). These results confirmed the strength of the Taguchi method's predictive ability because the optimum drilling parameter levels were determined for minimum D_f values. Thus, the optimal drilling parameter levels had been determined effectively and systematically and hole entry and hole exit damage was reduced by applying all stages of the Taguchi method in order to obtain minimum D_f values in the M1, M2, and M3 CFRP composite materials drilled with AWJ.

Table 7 Predicted optimum and confidence interval calculation results, and confirmation experiment results for delamination factor

Df_u (Hole entry, upper surface)		Df_b (Hole exit, bottom surface)	
Predicted optimum (Df_opt) and confidence interval (Df_CI) results		Predicted optimum (Df_opt) and confidence interval (Df_CI) results	
(a) M1 CFRP			
Df_opt	1.109	Df_opt	1.075
Df_CI	±0.108	Df_CI	±0.063
Prediction tolerance range for Df	$1.001 \leq 1.109 \leq 1.217$	Prediction tolerance range for Df	$1.012 \leq 1.075 \leq 1.138$
Results for optimum levels of drilling parameters		*Results for optimum levels of drilling parameters*	
Optimum levels	$WP_4–F_1–L_1–D_2$	Optimum levels	$WP_4–F_1–L_1–D_2$
Df (Experimental)	1.080, ($S/N = -0.668$ dB)	Df (Experimental)	1.027, ($S/N = -0.231$ dB)
Df (Predicted)	1.059, ($S/N = -0.547$ dB)	Df (Predicted)	1.030, ($S/N = -0.290$ dB)
Residual and % ratio of residual	0.021, 1.94%	Residual and % ratio of residual	0.003, 0.29%
Confirmation test results		*Confirmation test results*	
Levels	$WP_4–F_4–L_1–D_3$	Levels	$WP_4–F_4–L_1–D_3$
Df (Experimental)	1.091, ($S/N = -0.756$ dB)	Df (Experimental)	1.055, ($S/N = -0.465$ dB)
Df (Predicted)	1.101, ($S/N = -0.827$ dB)	Df (Predicted)	1.065, ($S/N = -0.541$ dB)
Residual and % ratio of residual	0.01, 0.92%	Residual and % ratio of residual	0.01, 0.95%
Residual and % ratio of residual between optimum level result and confirmation test result		*Residual and % ratio of residual between optimum level result and confirmation test result*	
Residual and % ratio of residual (Experimental)	0.011, 1.02%	Residual and % ratio of residual (Experimental)	0.028, 2.73%
Residual and % ratio of residual (Predicted)	0.042, 3.97%	Residual and % ratio of residual (Predicted)	0.035, 3.40%
(b) M2 CFRP			
Df_opt	1.143	Df_opt	1.055
Df_CI	±0.221	Df_CI	±0.207
Prediction tolerance range for Df	$0.922 \leq 1.143 \leq 1.364$	Prediction tolerance range for Df	$0.848 \leq 1.055 \leq 1.262$
Results for optimum levels of drilling parameters		*Results for optimum levels of drilling parameters*	
Optimum levels	$WP_4–F_1–L_1–D_2$	Optimum levels	$WP_4–F_1–L_1–D_2$
Df (Experimental)	1.062, ($S/N = -0.522$ dB)	Df (Experimental)	0.980, ($S/N = 0.175$ dB)
Df (Predicted)	1.043, ($S/N = -0.516$ dB)	Df (Predicted)	0.969, ($S/N = 0.148$ dB)
Residual and % ratio of residual	0.019, 1.79%	Residual and % ratio of residual	0.011, 1.12%
Confirmation test results		*Confirmation test results*	
Levels	$WP_4–F_4–L_1–D_3$	Levels	$WP_4–F_4–L_1–D_3$
Df (Experimental)	1.130, ($S/N = -1.061$ dB)	Df (Experimental)	1.029, ($S/N = -0.247$ dB)
Df (Predicted)	1.515, ($S/N = -1.192$ dB)	Df (Predicted)	1.054, ($S/N = -0.428$ dB)
Residual and % ratio of residual	0.385, 34.07%	Residual and % ratio of residual	0.025, 2.43%
Residual and % ratio of residual between optimum level result and confirmation test result		*Residual and % ratio of residual between optimum level result and confirmation test result*	
Residual and % ratio of residual (Experimental)	0.068, 6.40%	Residual and % ratio of residual (Experimental)	0.049, 5.00%
Residual and % ratio of residual (Predicted)	0.47, 45.25%	Residual and % ratio of residual (Predicted)	0.085, 8.77%
(c) M3 CFRP			
Df_opt	1.087	Df_opt	1.071
Df_CI	± 0.094	Df_CI	± 0.062
Prediction tolerance range for Df	$0.993 \leq 1.087 \leq 1.181$	Prediction tolerance range for Df	$1.009 \leq 1.071 \leq 1.133$
Results for optimum levels of drilling parameters		*Results for optimum levels of drilling parameters*	
Optimum levels	$WP_4–F_1–L_1–D_2$	Optimum levels	$WP_4–F_1–L_1–D_2$
Df (Experimental)	1.057, ($S/N = -0.482$ dB)	Df (Experimental)	1.015, ($S/N = -0.129$ dB)
Df (Predicted)	1.042, ($S/N = -0.399$ dB)	Df (Predicted)	1.029, ($S/N = -0.283$ dB)
Residual and % ratio of residual	0.015, 1.42%	Residual and % ratio of residual	0.014, 1.38%
Confirmation test results		*Confirmation test results*	
Levels	$WP_4–F_4–L_1–D_3$	Levels	$WP_4–F_4–L_1–D_3$

Table 7　(continued)

Df_u (Hole entry, upper surface)		Df_b (Hole exit, bottom surface)	
Predicted optimum (Df_opt) and confidence interval (Df_CI) results		Predicted optimum (Df_opt) and confidence interval (Df_CI) results	
Df (Experimental)	1.080, (S/N = − 0.671 dB)	Df (Experimental)	1.058, (S/N = − 0.491 dB)
Df (Predicted)	1.088, (S/N = − 0.724 dB)	Df (Predicted)	1.065, (S/N = − 0.538 dB)
Residual and % ratio of residual	0.008, 0.74%	Residual and % ratio of residual	0.007, 0.66%
Residual and % ratio of residual between optimum level result and confirmation test result		*Residual and % ratio of residual between optimum level result and confirmation test result*	
Residual and % ratio of residual (Experimental)	0.023, 2.18%	Residual and % ratio of residual (Experimental)	0.043, 4.24%
Residual and % ratio of residual (Predicted)	0.046, 4.41%	Residual and % ratio of residual (Predicted)	0.036, 3.50%

3.4 Surface roughness

Average surface roughness is another quality characteristic determined in this study. The surface roughness of the holes drilled in the laminated and fiber-reinforced composites is an important output variable, and minimum values are desired for CFRP composites in AWJ drilling.

3.4.1 SEM observations and EDS analysis for surface roughness

In the experiments, SEM images were taken of the holes in order to see the effect of abrasive particles likely to be embedded in the material layer after AWJ drilling of the CFRP composites. The SEM images of the hole surfaces with the highest and lowest average surface roughness values obtained as a result of the experiments are shown in Fig. 8, in which the difference between the hole surfaces can be clearly seen. The highest average surface roughness value (2.708 μm) was obtained on the surface of the 14-mm-diameter hole in the AWJ drilling of the M2 CFRP under drilling parameters of 3600 bar water pressure, 3000 mm/min traverse feed rate, and 4 mm stand-off distance (Fig. 8a). In this study, R_a surface roughness values obtained from AWJ machining are lower than R_a surface roughness values obtained by other researchers, which they used traditional experimental research methods or experimental design methods [15, 18, 24, 25, 31, 35, 41, 44, 47]. Since the kinetic energy of the jet enables the cutting process to take place at lower water pressure, the etching effect was also low. For this reason, cracks had formed in the composite material [27, 31]. These cracks caused gaps between the layers binding the composite, allowing abrasive particles to penetrate these gaps, and their remaining shear energy was sufficient to cause more imperfections between the layers [27]. The size of the abrasive particles embedded in the deep, wide cracks along with the cracks in the hole surface caused the roughness to increase and the surface quality of the holes

(a)

(b)
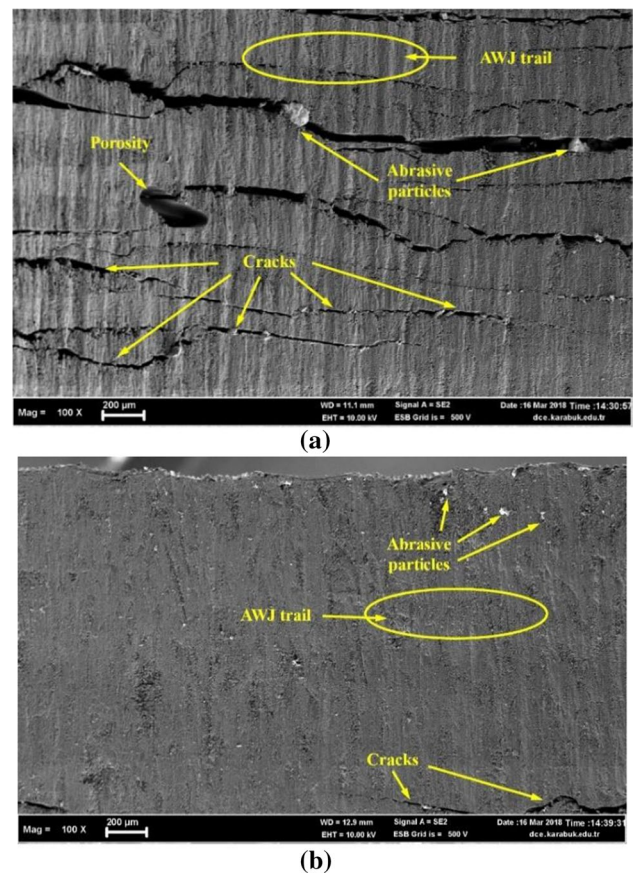
Fig. 8 SEM images of hole surfaces with the highest and lowest R_a values obtained as a result of AWJ drilling of CFRP composites: **a** $P = 3600$ bar, $F = 3000$ mm/min, $L = 4$ mm, $D = 14$ mm, **b** $P = 5300$ bar, $F = 3000$ mm/min, $L = 1$ mm, $D = 12$ mm

to deteriorate. Figure 8a shows abrasive particles that have penetrated the voids inside the cracks.

On the other hand, the lowest average surface roughness value (0.990 μm) was obtained on the surface of the 12-mm diameter hole in the AWJ drilling of the M2 CFRP under drilling parameters of 5300 bar water pressure, 3000 mm/min traverse feed rate, and 1 mm stand-off distance (Fig. 7b).

A decrease in the average surface roughness was observed with increasing water pressure and decreasing stand-off distance. This decrease in the average surface roughness value is similar to that reported in studies in the literature [15, 18, 24, 31, 36]. As the kinetic energy of the abrasive water jet rose with the increased water pressure ($P = 5300$ bar) and the lower stand-off distance ($L = 1$ mm), the effect of the force also rose. In addition, the cutting ability of the abrasive particles also increased with the increase in jet pressure [18]. Unde et al. [18] suggested using higher waterjet pressure for lower surface roughness values when cutting CFRP composites with AWJ. The higher abrasion force made it easier to wear the CFRP composite containing fiber. Since the material wear became easier to process, there was no opportunity for the abrasion force to cause deep and wide cracks in the hole surfaces. In addition, as the kinetic energy of the jet increased due to increased water pressure, the deflection of the jet to the cracks decreased, resulting in a decrease in the maximum crack length [23]. Since no deep or wide cracks occurred on the surface of the hole, abrasive particles could not become embedded into the crack by the jet. For all these reasons, the surface of the hole became smoother and better quality hole surfaces were obtained. Another reason that the average surface roughness values were low was that the hole diameter was smaller. Since the hole diameter radius will decrease with the reduction in the hole diameter, more water jet and particles in the water jet will be able to touch each cutting point during the cutting movement because of the lower bend radius. Therefore, in this case, a smooth surface will be obtained by providing easier cutting of the uncut fibers.

Water pressure is the most important process parameter for R_a surface roughness in drilling with AWJ, and the pressure of the water jet generates the cutting/abrasion force required for cutting. If the water pressure is too low, clean processing will not occur. The lower abrasion force caused by low jet pressure will disrupt the hole surface structure of the composite material. Figure 9 gives the variations of the average surface roughness depending on water pressure obtained in the AWJ drilling of the M1 CFRP composite under different machining conditions. As can be seen in this Fig. 9, at lower water pressure, deeper and wider cracks occurred and the number of cracks increased on the surface of the hole, which also reduced the quality of the hole surface.

As mentioned above and seen in Fig. 8a, due to the general process of the AWJ machining method, SEM images of the workpiece surface were taken for the detection of abrasives imbedded in the workpiece surface by the high pressure and kinetic energy as well as the deep cracks formed on the surface due to these abrasive particles (Fig. 10). In the $250\times$ magnification SEM image of the M1 CFRP composite given in Fig. 10, the element identification was performed by energy-dispersive X-ray spectroscopy (EDS) analysis. In the SEM image given in Fig. 10, object "1" is the M1 CFRP composite material (test sample), and object "2" is the abrasive (garnet) material. As a result of the EDS analysis, the element distribution of the object indicated by number "1" is shown in Fig. 11a, and the element distribution of object number "2" is shown in Fig. 11b. Figure 11a shows that C (carbon) has the highest peak value. This indicates that object "1" is the CFRP composite material. Figure 11b
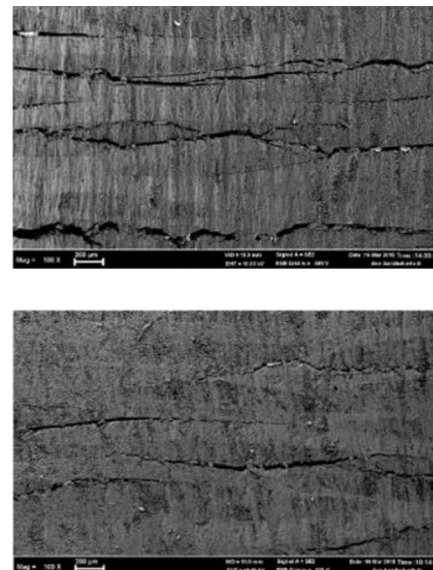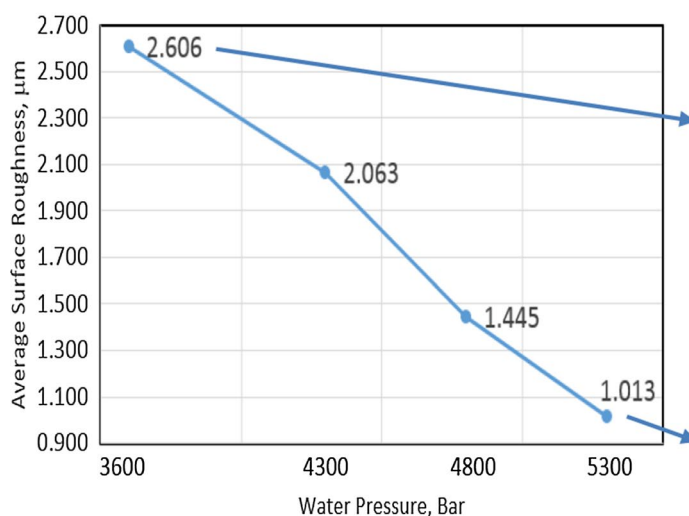
Fig. 9 The variation of average surface roughness values obtained by drilling the M1 CFRP composite with AWJ under different machining conditions depending on water pressure

Fig. 10 SEM image (WP = 3600 bar, F = 750 mm/min, L = 1 mm, D = 10 mm) of the M1 CFRP composite for EDS analysis of objects "1" and "2" after AWJ drilling
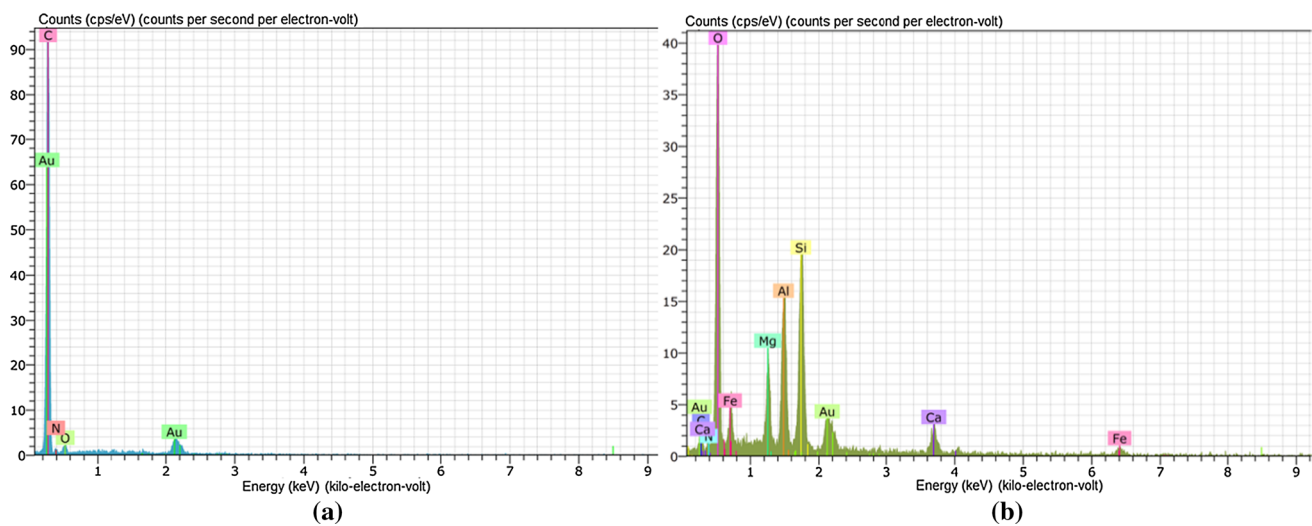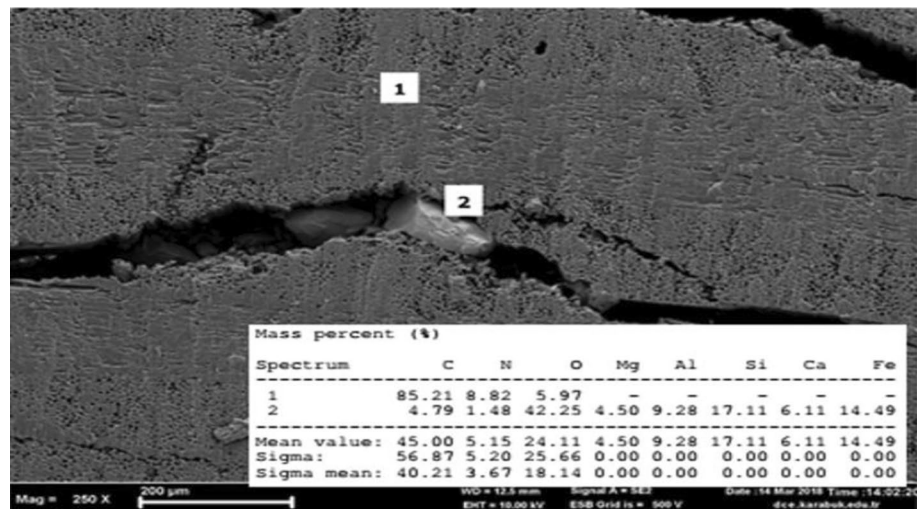
Fig. 11 EDS analysis and % distribution of elements: **a** CFRP composite material ("1"), **b** abrasive particle ("2")

shows that O (oxygen) is at the highest peak and that Si (silicon), Al (aluminum), Mg (magnesium), Au (gold), Fe (iron), Ca (calcium), and C (carbon) are also included among the elements, thus indicating that object "2" is garnet material.

3.4.2 Main effects of AWJ process parameters on surface roughness

The average surface roughness values calculated in Table 4 and the S/N ratio response tables for these surface roughness values are presented in Table 8, which shows that the most effective parameter on surface roughness is water pressure. The effect order of the control factors on surface roughness in AWJ drilling of the M1 and M2 CFRP composites was water pressure, stand-off distance, hole diameter, and traverse feed rate (Table 8a, b). For the M3 CFRP composites, this order was water pressure, stand-off distance, traverse

feed rate, and hole diameter (Table 8b). The optimum levels of AWJ drilling parameters for minimum R_a surface roughness in AWJ drilling of the M1, M2, and M3 CFRPs were identified as WP_4–F_3–L_1–D_2, WP_4–F_1–L_1–D_2, and WP_4–F_1–L_1–D_1, respectively. In Table 6a–c, optimum levels of AWJ drilling parameters are marked with "a". The optimum levels of drilling parameters for minimum R_a surface roughness were determined as P = 5300 bar, F = 2000 mm/min, L = 1 mm, and D = 10 mm for AWJ drilling of M1 CFRP; P = 5300 bar, F = 750 mm/min, L = 1 mm, and D = 10 mm for AWJ drilling of M2 CFRP, and P = 5300 bar, F = 750 mm/min, L = 1 mm, and D = 8 mm for AWJ drilling of M3 CFRP via Table 2, respectively.

The main effect plots that indicate the effects of AWJ drilling parameters on R_a surface roughness with S/N ratios are presented in Fig. 12, which shows the variation in R_a surface roughness depending on the order of action and level of

Table 8 Response table for means and signal-to-noise (*S/N*) ratios for average surface roughness

| S/N ratios for R_a (dB)					Means for R_a (µm)				
Level	A (*WP*)	B (*F*)	C (*L*)	D (*D*)	Level	A (*WP*)	B (*F*)	C (*L*)	D (*D*)
(a) M1 CFRP									
1	− 7.283	− 4.550	− 3.276[a]	− 4.619	1	2.322	1.716	1.520[a]	1.735
2	− 5.653	− 4.714	− 3.948	− 4.050[a]	2	1.920	1.745	1.632	1.648[a]
3	− 3.413	− 4.029[a]	− 5.160	− 4.437	3	1.495	1.690[a]	1.854	1.748
4	− 1.317[a]	− 4.375	− 5.283	− 4.562	4	1.172[a]	1.758	1.902	1.777
Difference	5.966	0.685	2.007	0.569	Difference	1.150	0.067	0.382	0.129
Rank	1	3	2	4	Rank	1	4	2	3
(b) M2 CFRP									
1	− 7.602	− 4.448[a]	− 3.231[a]	− 4.664	1	2.412	1.694[a]	1.515[a]	1.740
2	− 5.106	− 4.501	− 3.919	− 4.166[a]	2	1.803	1.704	1.622	1.658[a]
3	− 3.166	− 4.154	− 4.994	− 4.231	3	1.445	1.716	1.832	1.724
4	− 1.533[a]	− 4.304	− 5.264	− 4.346	4	1.206[a]	1.752	1.897	1.744
Difference	6.069	0.347	2.033	0.498	Difference	1.206	0.058	0.383	0.086
Rank	1	4	2	3	Rank	1	4	2	3
(c) M3 CFRP									
1	− 7.1369	− 2.5784[a]	− 1.8733[a]	− 2.6070[a]	1	2.2995	1.3773[a]	1.2860[a]	1.3923[a]
2	− 4.0018	− 3.5241	− 2.9141	− 2.9735	2	1.5878	1.5747	1.4953	1.5095
3	− 1.3384	− 2.9575	− 3.4357	− 3.4332	3	1.1765	1.5180	1.5708	1.5748
4	0.2518[a]	− 3.1653	− 4.0023	− 3.2116	4	0.9722[a]	1.5660	1.6840	1.5595
Difference	7.3887	0.9458	2.1290	0.8262	Difference	1.3273	0.1975	0.3980	0.1825
Rank	1	3	2	4	Rank	1	3	2	4

[a]Optimum level

each process parameter. It can be seen from Fig. 12a–c that water pressure was the most effective parameter in the AWJ drilling of composites with three different fiber orientation angles. With increasing water pressure, R_a surface roughness values decreased and hole surface quality improved [31, 35, 36, 40, 44, 46]. This was due to the kinetic energy of the water jet using abrasive particles at high pressure that enabled the cutting/abrasion force to cut more easily without creating deep cracks on the hole surface. The abrasive particles in the water jet were not embedded in deep, wide cracks and thus, the hole surface was smoother. Surface roughness values increased slowly due to the increase in the traverse-feed rate [29, 31, 35, 37, 44, 46]. In the study conducted by Alberdi et al., the most effective parameter on the surface roughness of CFRP/Ti6Al4V stacks was the traverse feed rate, followed by the stack configuration and water pressure. The increase in surface roughness values due to the traverse feed rate increase was attributed to the reduction in the exposure time created by the water jet [15, 29]. Traverse feed rate affects the time it takes to cut the material. With increase in the traverse feed rate, the abrasive particle has less time to cut the material and new particles are introduced to the cutting zone. However, the particles have more or less shear energy [18]. In addition, a reduction in the traverse feed rate

of the jet increases the abrasive mass flow rate per unit area, resulting in an increased cutting action. Consequently, the depth of cut increases and fewer particles penetrate into the cracks [23, 35]. An increase in the traverse feed rate causes the processing action to overlap less and the abrasive fewer particles to hit the surface. As a result, the surface roughness increases. With a decrease in the traverse feed rate, more abrasive particles strike the surface and consequently cause a decrease in roughness [31, 35, 36, 44]. Surface quality deteriorated with the increase in stand-off distance in the drilling of all three CFRP composites [24, 36, 37, 40]. As the stand-off distance increases, the distance travelled by the abrasive particles also increases. As the distance increases, the cutting ability of the abrasive particles caused by the kinetic energy will decrease, making it impossible to make sharp cuts in the material [40]. In other words, as the distance travelled (stand-off distance) increases, abrasive particles lose their cutting ability during travel. Moreover, a higher stand-off distance causes the jet to deviate before hitting the surface. Thus, the diameter of the jet increases when cutting is initiated. This results in decreased density in the kinetic energy of the jet due to its high interaction volume. Higher kinetic energy is preferred to achieve better penetration capability so that the jet can cut the material easily,
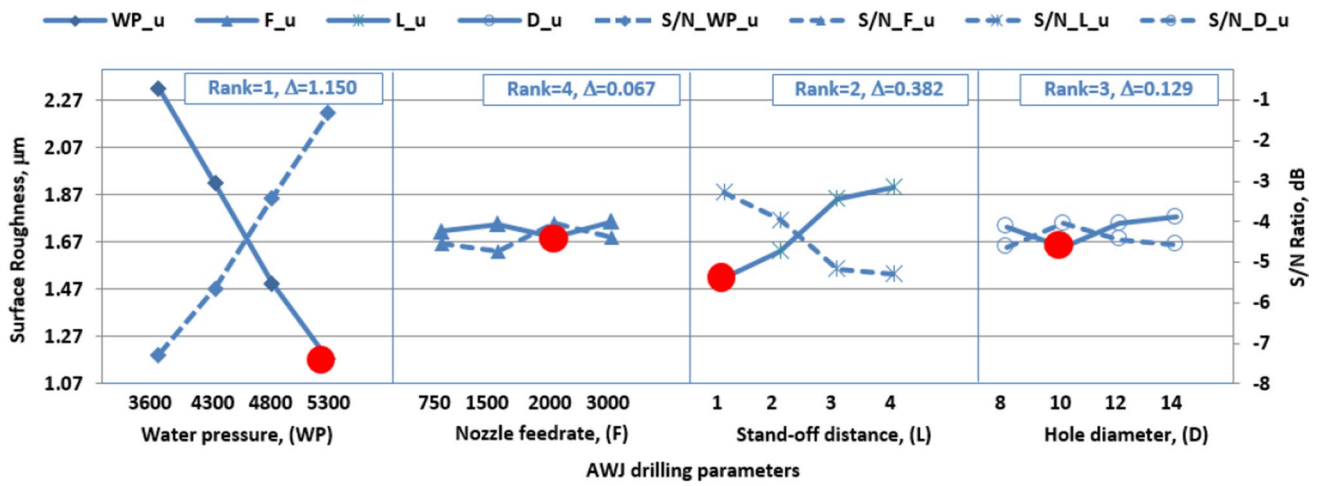
(a) M1 CFRP
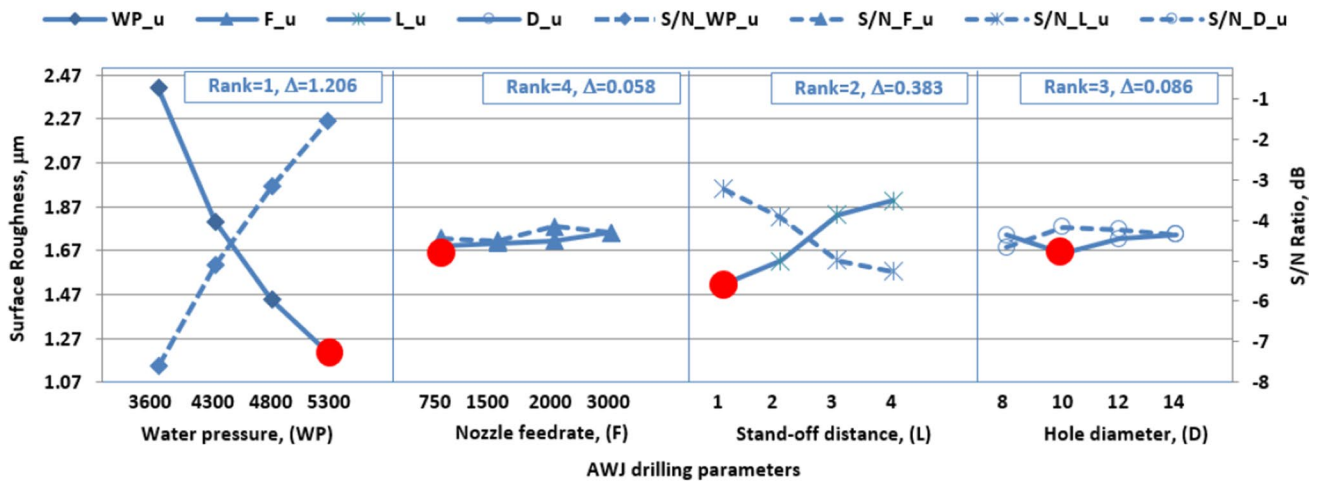
(b) M2 CFRP
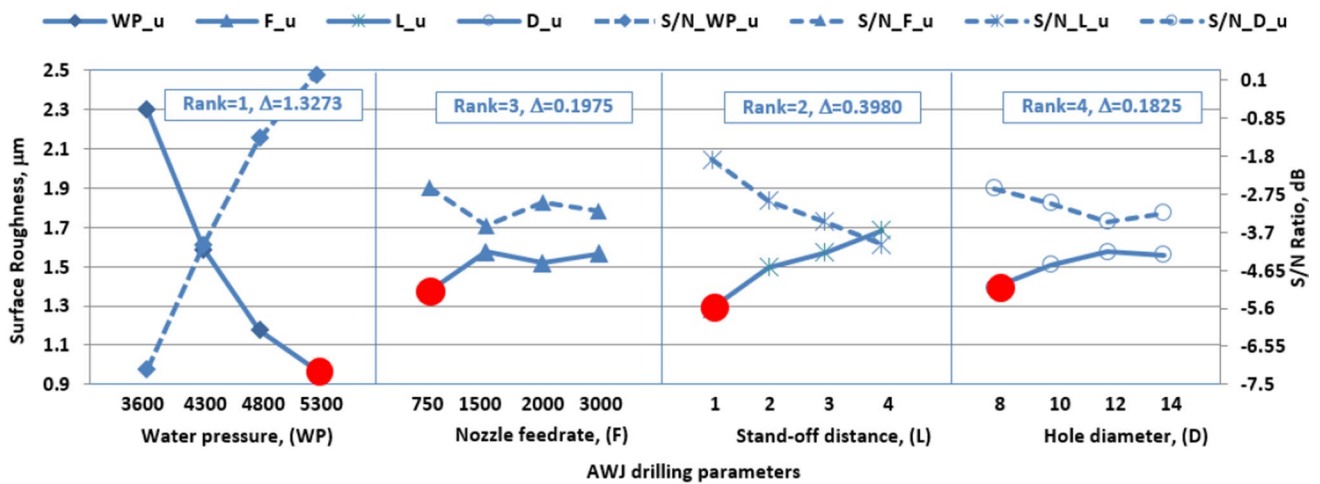
(c) M3 CFRP

Fig. 12 Main effects of AWJ drilling parameters on surface roughness

thus providing a smoother surface. Therefore, better surface quality is obtained with lower stand-off distance values [29]. The effect of stand-off distance on surface roughness in this study is consistent with the findings of previous studies [18, 24, 35–37, 40, 46]. In the cutting of all three CFRP composites, lower surface roughness values were obtained in cuts with lower diameters (8 and 10 mm) (Fig. 12). The order of effects of the control factors also coincides with the findings of Table 8.

3.4.3 Analysis of variance (ANOVA) for surface roughness

The ANOVA results for hole R_a surface roughness in AWJ drilling of the M1, M2, and M3 CFRPs are presented in Table 9. The effect of water pressure on R_a surface roughness was about 87−88%, followed by stand-off distance with an effect range of approximately 7.2−11.4%. Since $P < 0.05$ at 95% confidence level, the traverse feed rate and hole diameter had no statistically significant effect on surface roughness. The individual effects of traverse feed rate and hole diameter were below 2% in the drilling of the CFRP composites with three different fiber orientation angles. Therefore, it would suffice to control the levels of the water pressure and stand-off distance parameters, respectively, in order to obtain minimum hole surface roughness in AWJ drilling of these CFRP materials. Water pressure and traverse feed rate were determined as the most effective parameters on surface roughness in AWJ machining of carbon epoxy composites in the study conducted by Dhanawade et al. The traverse feed rate effect (54.61%) was determined as the most effective parameter on surface roughness. Water pressure was the second effective parameter (30.84%) after traverse feed rate [31]. Traverse feed rate and water pressure were also identified as the most effective AWJ parameters in the machining of Ti/CFRP/Ti laminates [34]. The traverse feed rate (24.26%) was the most effective parameter in the machining of hybrid GFRP composites, followed by water pressure and stand-off distance with effects of 11.50% and 8.20% [41]. In the machining of Kevlar epoxy composites, traverse feed rate (46.90%) and water pressure (44.49%) were the most effective parameters on surface roughness, followed by stand-off distance (4.09%) [44]. In the machining of glass/epoxy composite laminates, water pressure was determined as the most effective parameter on surface roughness with an effect of 41.9% [48]. In AWJ drilling of M1, M2, and M2 CFRP composites, correlation coefficients (R^2, %) for R_a were calculated as 99.8%, 98.6%, and 99.3%, respectively (Table 9). The high R^2 calculated in the ANOVA indicated that the effects of AWJ drilling parameters on the surface roughness can be explained at a high reliability rate. In addition, RSD was calculated in ANOVA for R_a. RSD for R_a were calculated as 0.0506, 0.1336, and 0.1071%, respectively (Table 9). When the RSD is exactly 0, then the model fits the data

perfectly. Since the calculated RSD values for R_a are very close to 0, the models fit the data perfectly.

3.4.4 Predictive optimum values, confidence intervals, and confirmation tests for surface roughness

The predictive optimal R_a surface roughness value (R_a_opt) was calculated from Table 9 based on the determination of the effective parameters ($P < 0.05$) for the surface roughness R_a and the optimum combinations of the process parameters in Table 8. The results are presented in Table 10, where R_a_opt values for each CFRP composite material (M1, M2, and M3) are calculated using Eq. (6).

$$R_a\_opt = R_{am} + (WP - R_{am}) + (L - R_{am}) \qquad (6)$$

Here, R_{am} is the arithmetic mean of the measurement results for R_a (Table 4), WP and L are the values determined by the Taguchi method for the optimum levels calculated from Table 8 for water pressure and stand-off distance. The ANOVA analysis in Table 9 determined the effective WP and L values. In AWJ drilling of the M1 CFRP composite material, via Eq. (6) it was calculated as R_a_opt= 0.965 μm using only parameters with significant effects, the optimum levels of these drilling parameters (WP_4–F_3–L_1–D_2), and the minimum R_a surface roughness value (Table 10). The predictive optimum R_a_opt of each CFRP composite are also presented in Table 10. As the next step of the Taguchi method, the confidence intervals (R_a_CI) for experimental and calculated predictive optimum R_a values measured by the validation experiments are calculated using Eqs. (2) and (3) (Table 10). As can be seen from Table 10, the experimental and predictive optimum R_a values calculated for each CFRP composite remained within the upper and lower limits of the R_a_CI. However, it is possible to say that the predictive optimum R_a values calculated with the Taguchi method were more precise than the predictive optimum R_a values calculated with Eq. (6) (Table 10) because the effects of all process parameters were taken into account in determining the predictive optimum R_a values calculated by the Taguchi method (e.g., 0.849 μm < 0.965 μm for M1 CFRP). Each CFRP composite material was subjected to confirmation tests by drilling at the optimal drilling parameter levels determined for them to obtain minimum R_a and under conditions not included in the experimental design in Table 4 (WP_4–F_4–L_1–D_3). For each CFRP's (M1, M2 and M3) R_a values, the residuals (relative error) between the R_a values obtained by the experiment performed at optimal levels of the AWJ drilling parameters and the predictive R_a value calculated by the Taguchi method and the % ratio of residuals (% ratio of relative error) were calculated and these are presented in Table 10a–c. The residuals for the R_a values of M1, M2, and M3 CFRP were obtained as 0.041 μm, 0.022 μm, and 0.029 μm, respectively. The

Table 9 Analysis of variance for average surface roughness

Source	Degree of freedom	Sum of square	Mean square	F-ratio	Prob. $> F$	Contribution %
(a) M1 CFRP						
A (WP)	3	3.01469	1.00490	392.63	0.000[a]	87.0
B (F)	3	0.01075	0.00358	1.40	0.394	0.3
C (L)	3	0.39477	0.13159	51.41	0.004[a]	11.4
D (D)	3	0.03688	0.01229	4.80	0.115	1.1
Error	3	0.00768	0.00256			0.2
Total	15	3.46477				100.0
$S=0.05059$, RSD$=0.0506$, $R^2=99.8\%$, R^2(adj)$=98.9\%$						
(c) M3 CFRP						
A (WP)	3	4.11899	1.37300	119.77	0.001[a]	88.1
B (F)	3	0.10004	0.03335	2.91	0.202	2.1
C (L)	3	0.33742	0.11247	9.81	0.046[a]	7.2
D (D)	3	0.08202	0.02734	2.38	0.247	1.8
Error	3	0.03439	0.01146			0.7
Total	15	4.67287				100.0
$S=0.1071$, RSD$=0.1071$, $R^2=99.3\%$, R^2(adj)$=96.3\%$						
(b) M2 CFRP						
A (WP)	3	3.30065	1.10022	61.62	0.003[a]	87.7
B (F)	3	0.00786	0.00262	0.15	0.925	0.2
C (L)	3	0.38300	0.12767	7.15	0.070[a]	10.2
D (D)	3	0.01910	0.00637	0.36	0.790	0.5
Error	3	0.05356	0.01785			1.4
Total	15	3.76416				100.0
$S=0.1336$, RSD$=0.1336$, $R^2=98.6\%$, R^2(adj)$=92.9\%$						

[a]Parameter with statistically significant effect, $P<0.05$

Table 10 Predicted optimum and confidence interval calculation results and confirmation experiment results for R_a

Predicted optimum (R_a_opt) and confidence interval (R_a_CI) results		Predicted optimum (R_a_opt) and confidence interval (R_a_CI) results	
(a) M1 CFRP		(b) M2 CFRP	
R_a_opt	0.965 μm	R_a_opt	1.004 μm
R_a_CI	± 0.178 μm	R_a_CI	± 0.471 μm
Prediction tolerance range for R_a	0.787 μm ≤ 0.965 μm ≤ 1.143 μm	Prediction tolerance range for R_a	0.533 μm ≤ 1.004 μm ≤ 1.475 μm
Results for optimum levels of drilling parameters		*Results for optimum levels of drilling parameters*	
Optimum levels	WP_4–F_3–L_1–D_2	Optimum levels	WP_4–F_1–L_1–D_2
R_a (Experimental)	0.890 μm, (S/N = 1.012 dB)	R_a (Experimental)	0.900 μm, (S/N = 0.915 dB)
R_a (Predicted)	0.849 μm, (S/N = 0.579 dB)	R_a (Predicted)	0.922 μm (S/N = − 0.320 dB)
Residual and % ratio of residual	0.041 μm, 4.83%	Residual and % ratio of residual	0.022 μm, 2.44%
Confirmation test results		*Confirmation test results*	
Levels	WP_4–F_4–L_1–D_3	Levels	WP_4–F_4–L_1–D_3
R_a (Experimental)	1.013 μm, (S/N = − 0.108 dB)	R_a (Experimental)	0.990 μm, (S/N = 0.087 dB)
R_a (Predicted)	1.016 μm, (S/N = − 0.155 dB)	R_a (Predicted)	1.048 μm, (S/N = − 0.244 dB)
Residual and % ratio of residual	0.003 μm, 7.72%	Residual and % ratio of residual	0.058 μm, 5.86%
Residual and % ratio of residual between optimum level result and confirmation test result		*Residual and % ratio of residual between optimum level result and confirmation test result*	
Residual and % ratio of residual (Exp.)	0.123 μm, 13.82%	Residual and % ratio of residual (Exp.)	0.090 μm, 10.00%
Residual and % ratio of residual (Pred.)	0.167 μm, 19.67%	Residual and % ratio of residual (Pred.)	0.126 μm, 13.67%
(c) M3 CFRP			
R_a_opt	0.836 μm		
R_a_CI	± 0.377 μm		
Prediction tolerance range for R_a	0.459 μm ≤ 0.836 μm ≤ 1.213 μm		
Results for optimum levels of drilling parameters			
Optimum levels	WP_4–F_1–L_1–D_1		
R_a (Experimental)	0.530 μm, (S/N = 5.514 dB)		
R_a (Predicted)	0.501 μm, (S/N = 2.362 dB)		
Residual and % ratio of residual	0.029 μm, 8.79%		
Confirmation test results			
Levels	WP_4–F_4–L_1–D_3		
R_a (Experimental)	0.920 μm, (S/N = 0.724 dB)		
R_a (Predicted)	0.872 μm, (S/N = 0.948 dB)		
Residual and % ratio of residual	0.048 μm, 5.50%		
Residual and % ratio of residual between optimum level result and confirmation test result			
Residual and % ratio of residual (Exp.)	0.390 μm, 73.58%		
Residual and % ratio of residual (Pred.)	0.371 μm, 74.05%		

mean of residuals is 0.031 μm. The relative error % ratio for R_a values of M1, M2, and M3 CFRP were obtained as 4.83%, 2.44%, and 8.79%, respectively. The mean of % ratio of residuals is 5.35%. Similarly, for each CFRP's (M1, M2 and M3) R_a values, the residuals (relative error) between the R_a values obtained by the experiment performed at optimal levels of the AWJ drilling parameters and the R_a value obtained by the confirmation test performed at different levels of the AWJ drilling parameters (WP_4–F_4–L_1–D_3) and the

% ratio of residuals (% ratio of relative error) were calculated and these are presented in Table 10a–c. The residuals for the R_a values of M1, M2, and M3 CFRP were obtained as 0.123 μm, 0.090 μm, and 0.390 μm, respectively. The mean of residuals is 0.201 μm. The relative error % ratio for R_a values of M1, M2, and M3 CFRP were obtained as 13.82%, 10.00%, and 73.58%, respectively. The mean of % ratio of residuals is 32.47%. As a result of the confirmation tests, the minimum R_a values obtained were close to the optimal

predictive R_a values obtained at the optimal parameter levels determined by the Taguchi method (Table 10). These results confirmed the strength of the Taguchi method's predictive ability because the optimum drilling parameter levels were determined for minimum R_a values. Thus, all stages of the Taguchi method had been applied for the evaluation of R_a surface roughness measurement results, the optimal levels of the parameters were determined in the AWJ drilling of M1, M2, and M3 CFRP composite materials, and the surface quality of the holes had been improved [31, 34].

4 Conclusions

In this experimental study, the effect of process parameters on the hole entry (upper surface) and the hole exit (bottom surface) delamination factor and R_a surface roughness were investigated in the AWJ drilling of M1, M2, and M3 CFRP composites having three different fiber orientations (M1: $[0°/90°]_s$, M2: $[+45°/-45°]_s$ and M3: $[0°/45°/90°/-45°]_s$). The optimum levels of the drilling parameters were determined for the minimum delamination factor and R_a surface roughness values. Since the M1, M2, and M3 CFRP composites had different fiber orientations, the effects of different fiber orientation angles on the delamination factor and surface roughness in AWJ processing were also determined in this study. The results were as follows:

1. In the AWJ drilling of CFRP composites, delamination occurred in the form of peeling outwards at the hole inlet and hole outlet.
2. For all CFRP composites with three different fiber orientation angles, the hole entry delamination formation was greater than that of the hole exit.
3. The average delamination factor for all CFRP composites was 1.160. The maximum delamination factor was 1.572 and the minimum was 1.029, which was obtained in the AWJ drilling of the M2 CFRP composite with $[+45°/-45°]$s fiber orientation angle,
4. The maximum difference (10.07%) between hole entry and hole exit delamination formation was observed in the AWJ drilling of the M2 CFRP composite with $[+45°/-45°]$s fiber orientation angle.
5. The most effective (66.6–82.4%) AWJ drilling parameter on the delamination factor was water pressure. No statistically significant effect ($P > 0.05$) of other parameters could be detected.
6. The hole entry and hole exit delamination factor values decreased with the increase in water pressure values. By increasing the water pressure, hole damage due to delamination formation was reduced.

7. The optimum process parameter levels to achieve minimum delamination formation at the hole inlet and outlet in the AWJ drilling of M1, M2, and M3 CFRP composites were: $WP = 5300$ bar, $F = 750$ mm/min, $L = 1$ mm, and $D = 10$ mm.
8. An average surface roughness value of 1.622 μm R_a was obtained in the drilling of the CFRP composites. The best hole surface quality (average 1.422 μm) was achieved in the AWJ drilling of the M3 CFRP $[0°/45°/90°/-45°]_s$ composite, and the worst surface quality (average 1.727 μm) in the M1 CFRP $[0°/90°]_s$ composite.
9. The highest average surface roughness value (2.708 μm) was obtained on the surface of the 14 mm-diameter hole in the AWJ drilling of the M2 CFRP composite with 3600 bar water pressure, 3000 mm/min traverse feed rate, and 4 mm stand-off distance, while the lowest average surface roughness value (0.990 μm) was obtained on the surface of the 12-mm diameter hole in the M2 CFRP composite with 5300 bar water pressure, 3000 mm/min traverse feed rate, and 1 mm stand-off distance.
10. Cracks, abrasive particles embedded in wide, deep cracks, and abrasive particles adhered to the surface were detected on the surface of the holes with high R_a surface roughness values. Deep cracks and abrasive particles adhered to/embedded in the hole surface were the reason for the reduced hole surface quality. Although no deep cracks were detected on the surface of the holes with low R_a surface roughness values, abrasive particles were found adhered to the hole surface.
11. The most effective parameter on surface roughness was water pressure, followed by stand-off distance in the AWJ machining of the M1 and M2 CFRP composites.
12. The statistically most significant effective (87.0–88.1%) AWJ drilling parameter on surface roughness was water pressure, followed by stand-off distance (7.2–11.4%). No statistically significant effect ($P > 0.05$) could be detected for other parameters.
13. Optimum parameters for minimum R_a average surface roughness in the AWJ drilling of M1, M2, and M3 CFRP composites were: WP_4–F_3–L_1–D_2 ($P = 5300$ bar, $F = 2000$ mm/min, $L = 1$ mm, and $D = 10$ mm), WP_4–F_1–L_1–D_2 ($P = 5300$ bar, $F = 750$ mm/min, $L = 1$ mm, and $D = 10$ mm), and WP_4–F_1–L_1–D_1 ($P = 5300$ bar, $F = 750$ mm/min, $L = 1$ mm, and $D = 8$ mm), respectively.
14. Predictive optimum values and confidence intervals were calculated for the delamination factor and R_a surface roughness, chosen as the quality characteristics. The experimental delamination factor and R_a surface roughness values obtained in the verification experi-

ments were quite close to the predictive values calculated with the Taguchi method. In this study, by using the Taguchi method, optimum drilling parameter levels were determined using a systematic approach, resulting in reduction in hole entry and hole exit damage and improvement in hole surface quality.

The findings of this study will contribute to the production of higher quality parts manufactured via AWJ machining of CFRP composites with different fiber orientation angles. When these optimum process parameter levels are applied in AWJ process planning for CFRP composites, minimum delamination formation and very good surface quality can be achieved.

References

1. Chung DD (2010) Composite materials: science and applications. Springer, Berlin
2. Leone C, Genna S, Tagliaferri V (2014) Fibre laser cutting of CFRP thin sheets by multi-passes scan technique. Opt Lasers Eng 53:43–50
3. Arul S et al (2006) The effect of vibratory drilling on hole quality in polymeric composites. Int J Mach Tools Manuf 46(3–4):252–259
4. Gaitonde V et al (2008) Analysis of parametric influence on delamination in high-speed drilling of carbon fiber reinforced plastic composites. J Mater Process Technol 203(1):431–438
5. Guu YH et al (2001) Effect of electrical discharge machining on the characteristics of carbon fiber reinforced carbon composites. J Mater Sci 36(8):2037–2043
6. Arisawa H, Akama S, Niitani H (2012) High-performance cutting and grinding technology for CFRP (carbon iber reinforced plastic). Mitsu Heavy Ind Tech Rev 49(3):3–9
7. Shukla M, Davim J Paulo (2013) Nontraditional machining processes, vol 39. Springer, Berlin
8. Davim JP, Reis P, Antonio CC (2004) Experimental study of drilling glass fiber reinforced plastics (GFRP) manufactured by hand lay-up. Compos Sci Technol 64(2):289–297
9. Drakonakis VM et al (2010) Matrix hybridization in the interlayer for carbon fiber reinforced composites. Polym Compos 31(11):1965–1976
10. Tsao C, Hocheng H (2007) Effect of tool wear on delamination in drilling composite materials. Int J Mech Sci 49(8):983–988
11. König W et al (1985) Machining of fibre reinforced plastics. CIRP Ann Manuf Technol 34(2):537–548
12. Kılıçkap E (2010) CETP Kompozitlerin Delinmesinde Oluşan Deformasyona Delme Parametrelerinin Etkisinin İncelenmesi. 2. Ulusal Tasarım İmalat ve Analiz Kongresi, p 77
13. Davim JP, Reis P (2003) Drilling carbon fiber reinforced plastics manufactured by autoclave-experimental and statistical study. Mater Des 24:315–324
14. Hashish M (2013) Trimming of CFRP aircraft components. In: 2013 WJTA-IMCA conference and expo, Houston, Texas
15. Alberdi A et al (2016) An experimental study on abrasive water-jet cutting of CFRP/Ti6Al4V stacks for drilling operations. Int J Adv Manuf Technol 86:691–704
16. Khashaba U (2004) Delamination in drilling GFR-thermoset composites. Compos Struct 63(3):313–327
17. Aich U et al (2014) Abrasive water jet cutting of borosilicate glass. Procedia Mater Sci 6:775–785
18. Unde PD et al (2015) Experimental investigations into abrasive waterjet machining of carbon iber reinforced plastic. J Compos 2015:1–9
19. Benedict GF (1987) Nontraditional manufacturing processes, vol 19. CRC Press, Boca Raton
20. Chung Y (1992) Development of prediction technique for the geometry of the abrasive waterjet generated kerf Dissertations 1154
21. Dittrich M et al (2014) Process analysis of water abrasive fine jet structuring of ceramic surfaces via design of experiment. Procedia Cirp 14:442–447
22. Hashish M (2014) Waterjet trimming and drilling of CFRP components for advanced aircraft. SME, 2014 technical paper
23. Shanmugam DK, Nguyen T, Wang J (2008) A study of delamination on graphite/epoxy composites in abrasive waterjet machining. Compos A Appl Sci Manuf 39(6):923–929
24. Phapale K et al (2016) Delamination characterization and comparative assessment of delamination control techniques in abrasive water jet drilling of CFRP. Procedia Manuf 5:521–535
25. Miron AV et al (2013) Studies on water jet cutting of 2D parts made from carbon iber composite materials. Acad J Manuf Eng 11(2):87–92
26. Wang J, Guo D (2002) A predictive depth of penetration model for abrasive waterjet cutting of polymer matrix composites. J Mater Process Technol 121(2):390–394
27. Mayuet PF et al (2015) SOM/SEM based characterization of internal delaminations of CFRP samples machined by AWJM. Procedia Eng 132:693–700
28. Miller J, Eneyew ED, Ramulu M (2013) Machining and drilling of carbon fiber reinforced plastic (CFRP) Composites. SAMPE J 49(2):36–47
29. Jagadeesh B et al (2018) Experimental investigation and optimization of abrasive water jet cutting parameters for the improvement of cut quality in carbon fiber reinforced plastic laminates. J Ind Text 48(1):178–200
30. Abidi A, Salem SB, Yallese MA (2019) Experimental and analysis in abrasive water jet cutting of carbon fiber reinforced plastics. In: 24ème Congrès Français de Mécanique. 2019: Brest, 26 au 30 Août
31. Dhanawade A, Kumar S (2019) Study on carbon epoxy composite surfaces machined by abrasive water jet machining. J Compos Mater 53(20):2909–2924
32. Dhanawade A, Kumar S (2017) Experimental study of delamination and kerf geometry of carbon epoxy composite machined by abrasive water jet. J Compos Mater 51(24):3373–3390
33. Dhanawade A, Kumar P, Kumar S (2020) Experimental study on abrasive water jet machining of carbon epoxy composite. Adv Mater Process Technol 6(1):40–53
34. Thongkaew K, Wang J, Li W (2019) An investigation of the hole machining processes on woven carbon-fiber reinforced polymers (CFRPs) using abrasive waterjets. Mach Sci Technol 23(1):19–38
35. Kumar D, Gururaja S (2020) Abrasive waterjet machining of Ti/CFRP/Ti laminate and multi-objective optimization of the

process parameters using response surface methodology. J Compos Mater 54(13):1741–1759

36. Vigneshwaran S, Uthayakumar M, Arumugaprabu V (2018) Abrasive water jet machining of fiber-reinforced composite materials. J Reinf Plast Compos 37(4):230–237

37. Kale SA (2019) Comprehensive evaluation of abrasive water jet machining of fiber reinforced polymers. J Polym Compos 7(1):7–16

38. Kim G, Denos BR, Sterkenburg R (2020) Influence of different piercing methods of abrasive waterjet on delamination of fiber reinforced composite laminate. Compos Struct 240:112065

39. Ramesha K et al (2019) Effect of the process parameters on machining of GFRP composites for different conditions of abrasive water suspension jet machining. Arab J Sci Eng 44(9):7933–7943

40. Prasad KS, Chaitanya G (2019) Experimental study on surface roughness and dimensional accuracy of hole machining process on GFRP composites using abrasive water jet technique. Mater Today Proc 23(3):651–658

41. Deepak D, Davim JP (2019) Multi-response optimization of process parameters in AWJ machining of hybrid GFRP composite by grey relational method. Procedia Manuf 35:1211–1221

42. Deepak D, Pai A (2019) Study on abrasive water jet drilling for graphite filled glass/epoxy laminates. J Mech Eng Sci 13(2):5126–5136

43. Li M et al (2019) Experimental study on hole characteristics and surface integrity following abrasive waterjet drilling of Ti6Al4V/CFRP hybrid stacks. Int J Adv Manuf Technol 104(9–12):4779–4789

44. Kumar P, Kant R (2019) Experimental study of abrasive water jet machining of Kevlar epoxy composite. J Manuf Eng 14(1):026–032

45. Gupta K (2020) Abrasive water jet machining of ceramic composites. In: Jagadish, Gupta K (ed) Abrasive water jet machining of engineering materials. Springer, Cham, pp 51–71

46. Mohanraj A et al (2019) Parameter optimization of abrasive water jet machining in aluminium 6061 material. Int J Eng Sci 9(3):1–3

47. Sankar SS, Reddy MVK, Pandian RS (2019) Multi-objective optimization of process parameters in abrasive water jet machining by using VIKOR. i-Manager's J Future Eng Technol 14(4):39–47

48. Azmir MA, Ahsan AK (2009) A study of abrasive water jet machining process on glass/epoxy composite laminate. J Mater Process Technol 209(20):6168–6173

49. Karatas M, Gokkaya H, Nalbant M (2019) Optimization of machining parameters for abrasive water jet drilling of carbon fiber-reinforced polymer composite material using Taguchi method. Aircr Eng Aerosp Technol 92(2):128–138

50. Meltem AK, Motorcu AR, Gökkaya A (2020) Optimization of machining parameters for Kerf angle and roundness error in abrasive water jet drilling Of CFRP composites with different fiber orientation angles. J Braz Soc Mech Sci Eng 42:173